FABRICATION OF BIOPOLYMERIC NANOGELS USING
SUPRAMOLECULAR INTERACTIONS

by

Hazal İpek

B.S., Chemical Engineering, Boğaziçi University, 2013

Submitted to the Institute for Graduate Studies in

Science and Engineering in partial fulfillment of

the requirements for the degree of

Master of Science

Graduate Program in Chemistry

Boğaziçi University

2015

To my family

ACKNOWLEDGEMENTS

I would like to express my thanks to my thesis Advisor assoc. Prof. Amitav Sanyal for taking a chance on a lowly chemical engineering student. His guidance and patience have been invaluable to my research and I am very grateful for his help, comments and support.

I would like to thank Assoc. Prof. Rana Sanyal for her all valuable advice regarding both research and life.

I would like to thank Prof. Faruk Yılmaz for his careful and constructive review of the final manuscript.

I'm very thankful to Yavuz Öz and Hasan Can Helvacı for helping me with TEM measurements. I would also like thank my labmates past and present: Janset, Sesil, Harun, Burcu, Filiz, Tuğçe, Özlem, Merve, Laura, Mehmet, Özgül, Duygu, Nergiz, Sadık, Yasemin, Evrim, Azize, Gizem, Büşra, Buğra, İsmail, Bianca and Suzan for always answering even the most inane of my questions, and giving me their friendship and support. They are some of the greatest people I have ever met and I have learned so much from all of them both in and out of the lab.

I would also like to thank my family for always believing in me more than I believe in myself and supporting me throughout my education.

ABSTRACT

FABRICATION OF BIOPOLYMERIC NANOGELS USING SUPRAMOLECULAR INTERACTIONS

In this study, biodegradable nanogels were fabricated using supramolecular host-guest type interactions between a βCD-grafted dextran polymer and disulfide-containing bis-adamantane based linkers. These nanogels were designed to exhibit redox-responsive diassembly when exposed to reducing agents such as glutahione and dithiothreitol (DTT). First generation nanogels were fabricated using the βCD-grafted dextran polymer and a disulfide-containing hydrophobic crosslinker. This combination resulted in formulation of extremely stable nanogels that could not be dissembled in the presence of DTT. It was postulated that the hydrophobic environment around the disulfide linker flanked between hydrophobic adamantane units did not allow efficient diffusion of the thiol-containing cleaving reagents. Hence a new hydrophilic crosslinker containing tetraethylene glycol (TEG) units was designed. Addition of a TEG unit between disulfide and adamantane moiety would overcome the steric and hydrophobic effects. Thus, second generation nanogels were fabricated using a disulfide-containing hydrophilic crosslinker and the βCD-grafted dextran polymer. As expected, these nanogels exhibited dissembly in the presence of DTT and glutathione. The effect of extent of βCD functionalization of dextran, polymer concentration and βCD to adamantane ratio on the size and reduction sensitivity of these nanogels were studied. An anti-cancer drug doxorubicin was loaded into the nanogels by either simple mixing or dialysis-based methods. The latter approach allowed control over size and produced stable nanogels with better drug loading capacites and loading efficiencies.

ÖZET

SUPRAMOLEKÜLER ETKİLEŞİMLER KULLANILARAK BİYOPOLİMERİK NANOJEL ÜRETİMİ

Bu çalışmada, βCD graft edilmiş dextran polimer ve disulfid bağı içeren bis-adamanten çapraz bağlayıcı arasındaki supramoleküler host-guest tipi etkileşimler kullanılarak biyobozunabilir nanojeller üretilmiştir. Nanojeller, glutation ve DTT gibi indirgeyici ajanlarlara maruz kaldığında redoks-responsif bozulma gösterecek şekilde tasarlanmıştır. Birinci nesil nanojeller βCD graft edilmiş dextran ve disülfid bağı içeren hidrofobik çapraz bağlayıcı kullanılarak üretilmiştir. Bu nanojeller DTT ile bozulma göstermeyecek kadar kararlı olmuşlardır. Buna neden olarak, disulfid bağı etrafındaki hidrofobik ortamın, tiyol içeren bağ kırıcı ajanların nanojele etkin bir şekilde difüze olmasını engellemesi öne sürülmüştür. Bu nedenle tetraetilen glikol (TEG) içeren yeni bir hidrofilik çapraz bağlayıcı sentezlenmiştir. Adamanten ve disulfid kısımları arasına eklenen TEGin, sterik ve hidrofobik etkilerin azalmasını sağlayacağı düşünülmüştür. Bu hidrofilik disulfid bağı içeren bağlayıcı ve βCD graft edilmiş dextran kullanılarak ikinci nesil nanojeller üretilmiştir. Beklendiği üzere ikinci nesil nanojeller DTT ve glutatiyon ile bozulma göstermiştir. Dextrana graft edilmiş βCD miktarı, polimer konsantrasyonu ve βCD-adamanten oranının nanojellerin boyutu ve redoks responsifliği üzerindeki etkisi incelenmiştir. Nanojellere, bir kanser ilacı olan doxorubicin karıştırma veya diyaliz yöntemleri ile yüklenmiştir. Diyaliz yöntemiyle üretilen nanojeller daha kararlı olup, kontol edilebilir boyutlara ve daha iyi iyi ilaç yükleme kapasitesi ve verimliliğine sahip olmuşlardır.

TABLE OF CONTENTS

LIST OF FIGURES

LIST OF TABLES

LIST OF SYMBOLS

J Coupling constant

LIST OF ACRONYMS/ABBREVIATIONS

AD	Adamantane
AHG	Anhydroglucose
DCC	N,N'-Dicyclohexylcarbodiimide
DCM	Dichloromethane
DLS	Dynamic Light Scattering
DLNG	Drug Loaded Nanogel
DMAP	4-Dimethylaminopyridine
DMF	N,N'-dimethyl formamide
DMSO	Dimethyl sulfoxide
DOX	Doxorubicin
DPTS	4-(dimethylamino)pyridinium-4-toluene sulfonate
DT40	Dextran (Molecular weight = 40 kDa)
DTT	Dithiothreitol
EDCI	1-Ethyl-3-(3-dimethylaminopropyl)carbodiimide
FT-IR	Fourier Transform Infrared
GSH	Glutathione
IPA	Isopropyl alcohol
MeOH	Methanol
NG	Nanogel
PDI	Polydispersity Index
PMDETA	N,N,N′,N′,N″-pentamethyldiethylenetriamine

RT   Room temperature

SEM   Scanning Electron Microscopy

TEA   Triethylamine

TEG   Tetraethylene glycol

TEM   Transmission Electron Microscopy

UV-Vis   Ultraviolet-Visible

βCD   Beta-cyclodextrin

1. INTRODUCTION

1.1. Supramolecular Chemistry

'Supramolecular chemistry' is the designed chemistry of the intermolecular bond, or "chemistry beyond the molecule." A supramolecular aggregate is formed by molecular building blocks (molecules or ions) held together by reversible non-covalent interactions. A summary of frequently utilized supramolecular interactions can be found in Table 1.1. Supramolecular chemistry is a highly interdisciplinary field of science covering organic and inorganic chemistry to synthesize precursors for supermolecules, physical chemistry to understand the properties of supramolecular systems and computational modelling to understand complex supramolecular behavior. Supramolecular systems are abundant in nature. A well known-example is DNA, which is made up of two strands in a double helix structure self-assembled via hydrogen bonds and aromatic stacking. Based on the chemical, physical, and biological features of existing supramolecular systems, novel lines of investigation have developed, concerned with the design of molecular devices and of systems displaying higher forms of molecular and supramolecular behavior such as self-organization, regulation, cooperativity, communication, and replication [1,2].

Table 1.1. Summary of supramolecular interactions [2].

Interaction	Strength (kJ mol^{-1})	Example
Ion-ion	200-300	Tetrabutylammonium chloride
Ion-dipole	50-200	Sodium [15]crown-5
Dipole-dipole	5-50	Acetone
Hydrogen bonding	4-120	DNA/RNA
Cation-π	5-80	K^+ in benzene
π-π	0-50	Benzene and graphite
van der Waals	<5, variable depending on surface area	Packing in molecular crystals
Hydrophobic	related to solvent-solvent interaction energy	Cyclodextrin inclusion complexes

Supramolecular chemistry can be broadly divided into two categories: host-guest chemistry and self-assembly, the main difference between them being size and scope.

1.1.1. Host-Guest Chemistry

Host-guest chemistry consists of two components that form a complex. The large "host" molecule is capable of enclosing smaller "guest" molecules via non-covalent interactions. Examples of host-guest chemistry can be found in biological systems, such as enzymes and their substrates; and in coordination chemistry, such as metal-ligand complexes where large (often macrocyclic) ligands act as hosts for metal cations. The selectivity of host-guest chemistry allows design and control of supramolecular systems specifically for a variety of applications: such as drug delivery, biological modelling, sensing, food additives and cosmetics. Host molecules can be macrocyclic (e.g. cyclodextrins) or acyclic.

1.1.2. Self-Assembly

Broadly, self assembly is the autonomous organization of components into patterns or structures without human intervention. The self-assembling processes common in nature and technology can have range from the molecular and planetary scale and make use of a variety of interactions. In terms of supramolecular chemistry it is the spontaneous and reversible association of molecules or ions via non-covalent interactions to form larger supramolecular aggregates under equilibrium conditions. The reversible nature of these systems allows for the correction of mistakes and formation of thermodynamically stable products by continuous association and disassociation. There are many processes in nature that rely on self-assembly: replication of DNA, folding of proteins and virus formation are a few examples. Taking inspiration from these processes and building on existing knowledge of what compounds may interact well together, it is possible to design systems of well defined size, shape and functionality in the nanoscale [2,3].

1.2. Cyclodextrins

Cyclodextrins (CD) are a family of macrocyclic oligosaccharides containing six (αCD), seven (βCD), eight (γCD) or more (α-1,4-)linked D-glucopyranose units (Figure 1.1). The commercial manufacturing process for the three most common CDs – αCD, βCD and γCD – consists of three steps: (1) Bacterial fermentation and extraction of CD glycosyltransferase. (2) Enzymatic CD production from starch and precipitation of CD

through complexation. (3) Removal of the complexing agent and product purification. Due to the chair conformation of the glucopyranose units, CDs are have a truncated cone shape with secondary hydroxy groups extending from the wider edge and the primary groups from the narrow edge. As a result of this, CDs have a hydrophilic outer surface and a hydrophobic cavity [4].
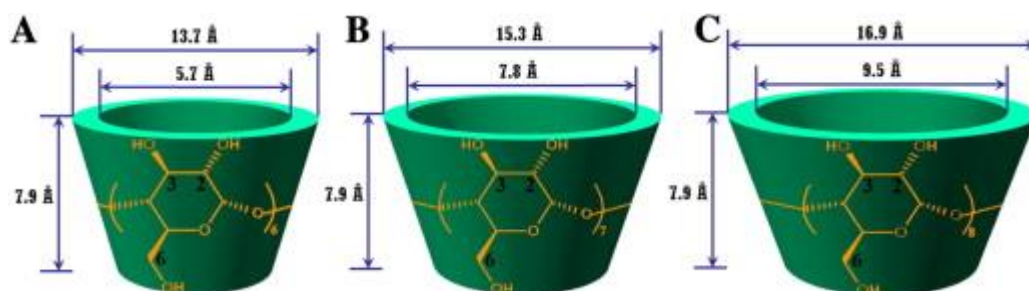
Figure 1.1. Molecular structures and dimesions of α-, β- and γCD [5].

This hydrophobic cavity allows CDs to form inclusion complexes with a variety of small organic molecules. Inclusion complex occurs when the water molecules inside the hydrophobic cavity are displaced by the hyrophobic guest or hydrophobic moiety of a larger molecule. The driving force of the complex formation is the substitution of the high-enthalpy water molecules in the hydrophobic cavity by a hyrophobic guest or hydrophobic moiety of a larger molecule. Most frequently the host:guest ratio is 1:1, however, 2:1, 1:2, 2:2, or even more complicated associations, and higher order equilibria also exist. Complex formation is characterized by the binding (or association) constant, which is the equilibrium constant for the reversible binding process. Below in Equation 1.1, the equilibrium of a 1:1 CD-guest system can be observed. The binding constant related to the complexation can be found in Equation 1.2 [2,6].

$$CD + G \leftrightarrow CD.G \qquad (1.1)$$

$$K_a = \frac{[CD][G]}{[CD.G]} \qquad (1.2)$$

Some binding constants for 1:1 complexation of α-, β- and γ-CDs with small organic guest molecules can be found in Table 1.2.

Table 1.2. Binding constants of α- to γ-CDs, studied by capillary electrophoresis [6].

Compound	K_a (M^{-1})		
	αCD	βCD	γCD
benzoic acid	16	23	3
2-methylbenzoic acid	13	13	7
3-methylbenzoic acid	26	40	6
4-methylbenzoic acid	36	66	8
2,4-dimethylbenzoic acid	45	42	8
3,5-dimethoxybenzoic acid	47	63	10
salicylic acid	11	65	13
3-phenylpropionic acid	35	79	7
4-*tert*-butylbenzoic acid	51	457	59
ibuprofen	55	2600	59
1-adamantanecarboxylic acid	114	1500	42

As mentioned above, CDs can form inclusion complexes with small organic molecules, such as drugs, and improve their water solubility as well as act as stabilizers for proteins and peptides [7]. In fact, CDs are among the most widely used components in host-guest chemistry. In addition, their easy production from a renewable natural source (starch), their wide availability, their facile modification through hydroxy groups on the periphery, their biodegradability and favorable toxicological profiles make CDs and their derivatives ideal candidates for biomedical applications [8]. A list of available pharmaceutical products containing cyclodextrins can be found in Table 1.3 below. CDs are also used in the food industry as stabilizers for flavoring agents, preparations of oil/water emulsions and removal of cholesterol from butter; cosmetic industry for increasing bioavailability of vitamins and emulsion preparation; and analytical chemistry for separation technologies such as thin layer chromatography, gas chromatography, capillary electrophoresis and high-performance liquid chromatography (HPLC) [2].

Table 1.3. Cyclodextrin containing pharmaceutical products as of 2005 [9].

Drug/cyclodextrin	Trade name	Formulation	Country
α-Cyclodextrin			
Alprostadil (PGE$_1$)	Prostavastin, Rigidur	I.V. solution	Japan, Europe, USA
OP-1206	Opalmon	Tablet	Japan
Cefotiam hexetil HCl	Pansporin T	Tablet	Japan
β-Cyclodextrin			
Benexate HCl	Ulgut, Lonmiel	Capsule	Japan
Cephalosporin (ME 1207)	Meiact	Tablet	Japan
Chlordiazepoxide	Transillium	Tablet	Argentina
Dexamethasone	Glymesason	Ointment	Japan
Diphenhydramin HCl, Chlortheophyllin	Stada-Travel	Chewing tablet	Europe
Iodine	Mena-Gargle	Solution	Japan
Nicotine	Nicorette, Nicogum	Sublingual tablet, chewing gum	Europe
Nimesulide	Nimedex	Tablet	Europe
Nitroglycerin	Nitropen	Sublingual tablet	Japan
Omeprazol	Omebeta	Tablet	Europe
PGE$_2$	Prostarmon E	Sublingual tablet	Japan
Piroxicam	Brexin, Flogene, Cicladon	Tablet, Suppository, Liquid	Europe, Brazil
Tiaprofenic acid	Surgamyl	Tablet	Europe
2-Hydroxypropyl-β-cyclodextrin			
Cisapride	Propulsid	Suppository	Europe
Itraconazole	Sporanox	Oral and I.V. solutions	Europe, USA
Mitomycin	Mitozytrex	I.V. infusion	Europe, USA
Methylated β-cyclodextrin			
Chloramphenicol	Clorocil	Eye drop solution	Europe
17β-Estradiol	Aerodiol	Nasal spray	Europe
Sulfobutylether β-cyclodextrin			
Voriconazole	Vfend	I.V. solution	Europe, USA
Ziprasidone mesylate	Geodon, Zeldox	IM solution	Europe, USA
2-Hydroxypropyl-γ-cyclodextrin			
Diclofenac sodium	Voltaren	Eye drop solution	Europe
Tc-99 Teoboroxime	Cardiotec	I.V. solution	USA

In the recent years, the main focus of CD research has been self-assembled systems ranging from the molecular-, to nano- and macro-scale that make use of inclusion complexation phenomena. Supramolecular block copolymers [10], self-assembled monolayers (SAMs) [11], polyrotaxanes [12], nanogels [13], nanofibers [14], micelles [15], polymeric vesicles [16], nanoparticles [17], microcapsules [18] and hydrogels [19] have all been widely investigated. These structures have found use in a wide array of applications, such as drug delivery [20], sensing [21] and self-healing materials [22]. Given below are a few examples of these supramolecular systems. For the purposes of this thesis, βCD will be the main focus.

The names and structures of some molecules commonly used as guests for βCD can be found in Figure 1.2. Adamantane is the most widely used guest molecule, as the inclusion complex formed has a very high binding constant which leads to stable structures. It is also possible to incorporate stimuli responsiveness into the systems by using azobenzene (UV-sensitive), benzimidazole (pH-sensitive) or ferrocene (redox-sensitive) as guests.
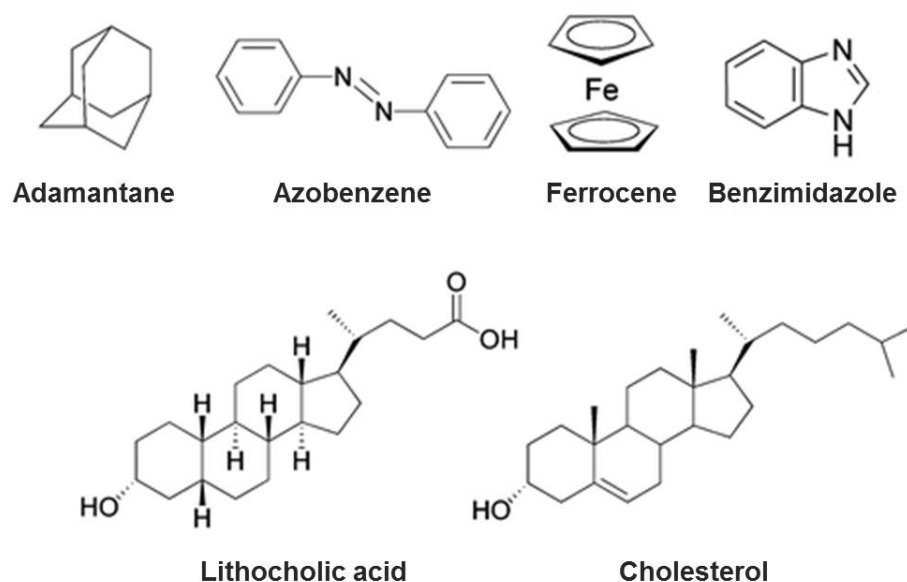
Figure 1.2. Some guest molecules for β-cyclodextrin, adapted from [23].

Li and coworkers reported a thermoresponsive psuedo block copolymer consisting of a βCD-core poly(N-isopropylacrylamide) (PNIPAAm) star polymer and adamantane modified poly(etylene glycol) (PEG) that form a supramolecular self assembly via inclusion complexation. It was found that the lower critical solution temperature (LCST) could be tuned by changing the ratio of adamantane to βCD and the length and structure of adamantane bearing PEG (Figure 1.3). These supramolecular block copolymer systems are advantageous over conventional block copolymer systems because the same βCD-core PNIPAAm star polymer can be combined with different guest molecules to achieve desired LCST [24].
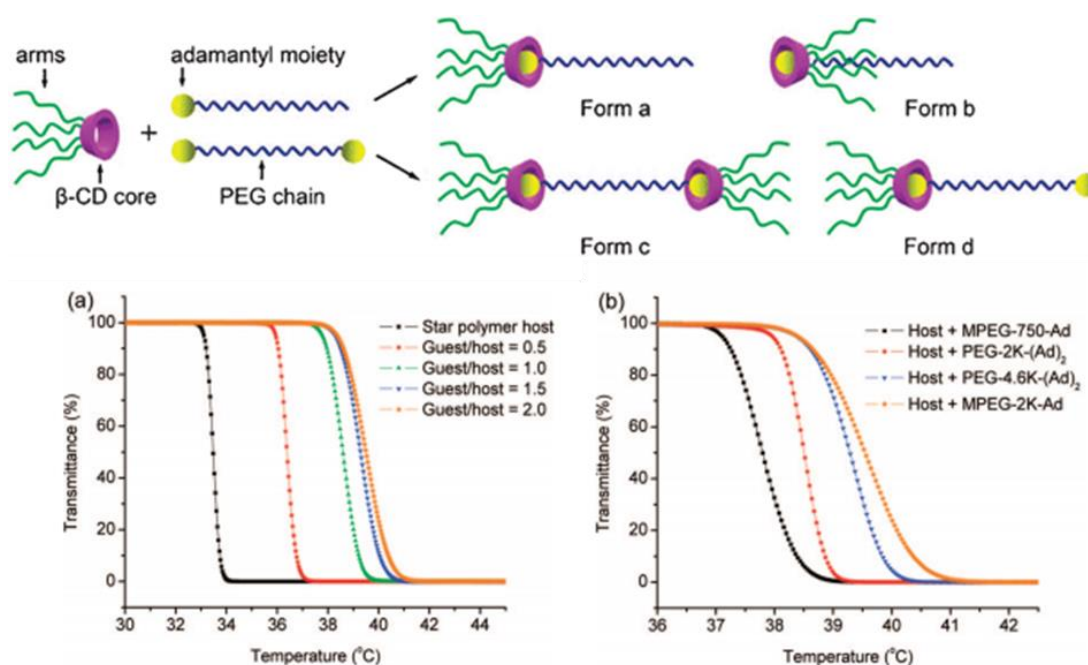
Figure 1.3. Different chain architectures of pseudo block copolymers composed of β-CD-core star PNIPAM and PEG via inclusion complexation (above) and thermoresponsive behavior of the systems (below) [24].

Harada and coworkers made use of the reversible nature of the inclusion complexes of CDs to design self-healing hydrogels. In this study, acrylamide based free standing hydrogels were synthesized by homogeneous radical copolymerization, using βCD-adamantane pair as in situ-formed crosslinkers at high mole ratios. After cutting and rejoining, the gels were able to be lifted against their own weight and did not produce cracks upon dropping. Adding a competitive guest (1-adamantane carboxylic acid sodium salt) to the cut surface prevented adhesion of two sides, demonstrating that self-healing

ability is due to host-guest interactions. (Figure 1.4) The change in adhesion strength after rejoining was also investigated as a function of adhesion time. It was found that the gel recovers 90% of its strength after 10 hours [25].
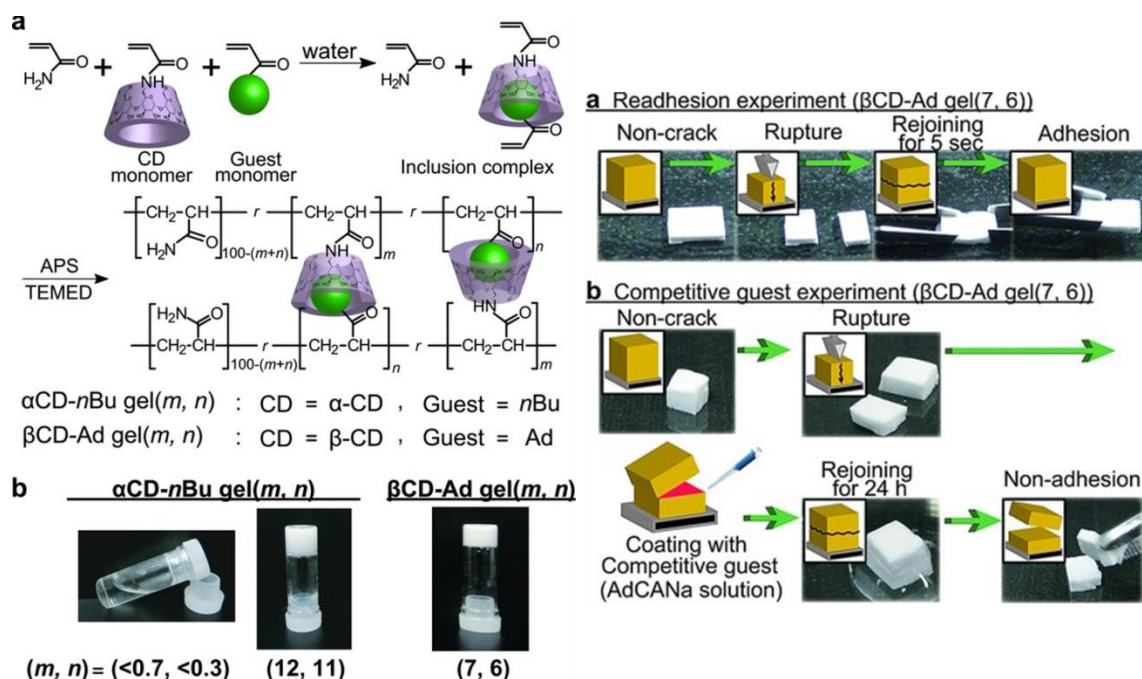
Figure 1.4. Preparation of host-guest supramolecular hydrogels (left) and photographs of self-healing experiments (right) [25].

For cancer therapy applications, designing drug delivery systems that would be responsive to the unique environment of tumor tissue while remaining stable in healthy tissue is of great importance. He, Chen and coworkers took advantage of the pH-sensitive inclusion complexation betwen βCD and benzimidazole (BM) to construct supramolecular blockamphiphiles which would form micelles that would disassemble at the low pH of tumor tissue. The amphiphile consist of two parts: βCD-terminated dextran (Dex- βCD) as the hydrophilic block and BM-terminated poly(ε-caprolactone) (BM-PCL) as the hydrophobic block. At physiological pH 7.4, BM forms a stable inclusion complex with βCD, however below pH 6, BM is protonated which causes the complex, and as a result the micelle, to dissociate (Figure 1.6). Doxorubicin (DOX), an anti-cancer drug, was physically loaded into the micelles and their release profiles were studied. As expected, drug release was faster in acidic conditions that mimicked endosomal conditions [26].
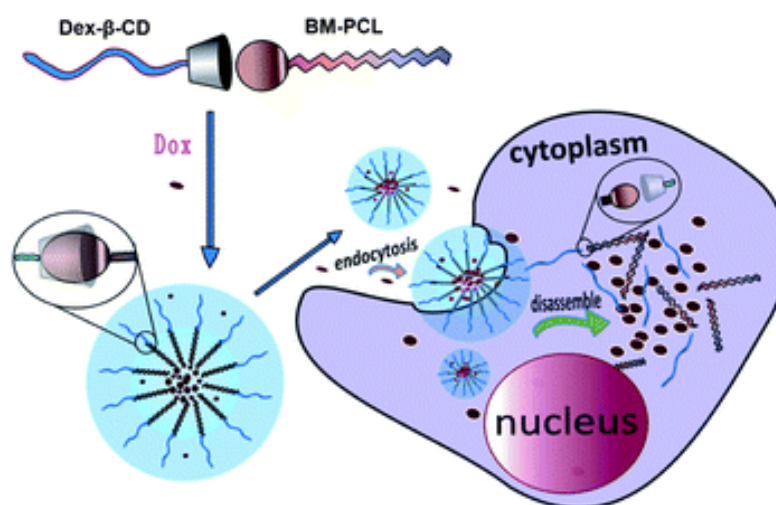
Figure 1.5. Dox loading and intracellular acidic pH-triggered release from DOX-loaded Dex-βCD/BM-PCL micelles [26].
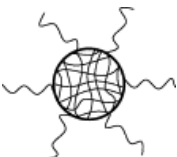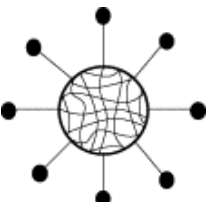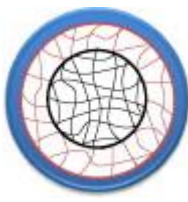
1.3. Nanogels

Nanogels are nano-sized (typically 20 nm to 250 nm) hydrogels made up of crosslinked hydrophilic polymers and water. They have high water content, high specific surface area, biocompatibility and stability [27]. Polymer chains can be linked to each other via weak interactions (physically crosslinked nanogels) or covalent interactions (chemically crosslinked nanogel). Nanogels make use of the advantages of both hydrogels and nanoscale size. Like hydrogels, nanogels can also can host, solubilize and protect drug molecules. If needed, the release of the drug molecules can be controlled by introducing high-affinity functional groups, stimuli-responsive conformations or biodegradable bonds into the polymer network. Their hydrophilicity allows them to be easily dispersed in aqueous media, making them suitable for administration in liquid dosage form. Their high specific surface area can be used for bioconjugation of active targeting agents. For these reasons, nanogels are well-suited to biomedical applications [28].

Nanogels can be obtained through bottom-up and top-down methods. In the bottom-up method, nanosized networks are produced directly from building blocks while in the top-down approach preformed macro-scale networks are broken down to nanosized structures [29]. The building blocks of the networks may be physical self-assembly of

interactive polymers, preformed polymer chains crosslinked covalently or by supramolecular interactions, monomers that simultaneously undergo polymerization and crosslinking reactions or template assisted nanofabrication of nanogel particles.

Table 1.4. Different structures of nanogels [30].

Type	Schematic structure	Type	Schematic structure
Nanogel		Core–shell nanogel	
Hairy nanogel		Hollow nanogel	
Functionalized nanogel		Multilayer nanogel	

As nanogels are highly tunable in terms of size, shape and functionality, Table 1.13 shows different structures of nanogels that can be produced. While their versatility make them ideal candidates for biomedical applications, there are some disadvantages of using of nanogels rather than other delivery systems. Namely, their limited drug loading efficiency and still suboptimal regulation of drug release. These limitations give rise to a search for moieties that possess high affinities for specific drugs and retain them through non-covalent interactions. However, strong drug–polymer interactions can decrease the nanogel's hydrophilicity and cause the nanogel structure to collapse, irreversibly entrapping the drug molecules within the shrunken structure and causing an unfavorable release profile [30]. Incorporating CDs into the nanogel structure strikes a balance between these two concerns, as they can form inclusion complexes with drug molecules while preserving the hydrophilicity of the nanogels.

1.3.1. β-Cyclodextrin Based Nanogels

As mentioned above, CDs can form inclusion complexes with small organic molecules, and non-inclusion complexes with proteins as peptides, which give them a

twofold purpose in nanogel structure: They can increase the loading content and efficiency of the nanogel. Also, they can contribute to the formation of the network via host-guest interactions in self-assembled nanogel systems. CDs can be introduced into the nanogel structure in three ways (1) key–lock interactions among preformed chains, with some bearing CDs and others possessing suitable guest moieties [31], (2) direct covalent crosslinking of CD units by condensation with suitable bi/multifunctional agents [32], (3) polymerization of CD monomers bearing acrylic or vinyl moieties [33]. As the focus of this thesis is self-assembled systems, only key-lock type nanogels will be examined further.

Figure 6. Schematic structures of the nanoassemblies formed with Ada grafted dextrans having (A) a lower Ada substitution degree than (B).
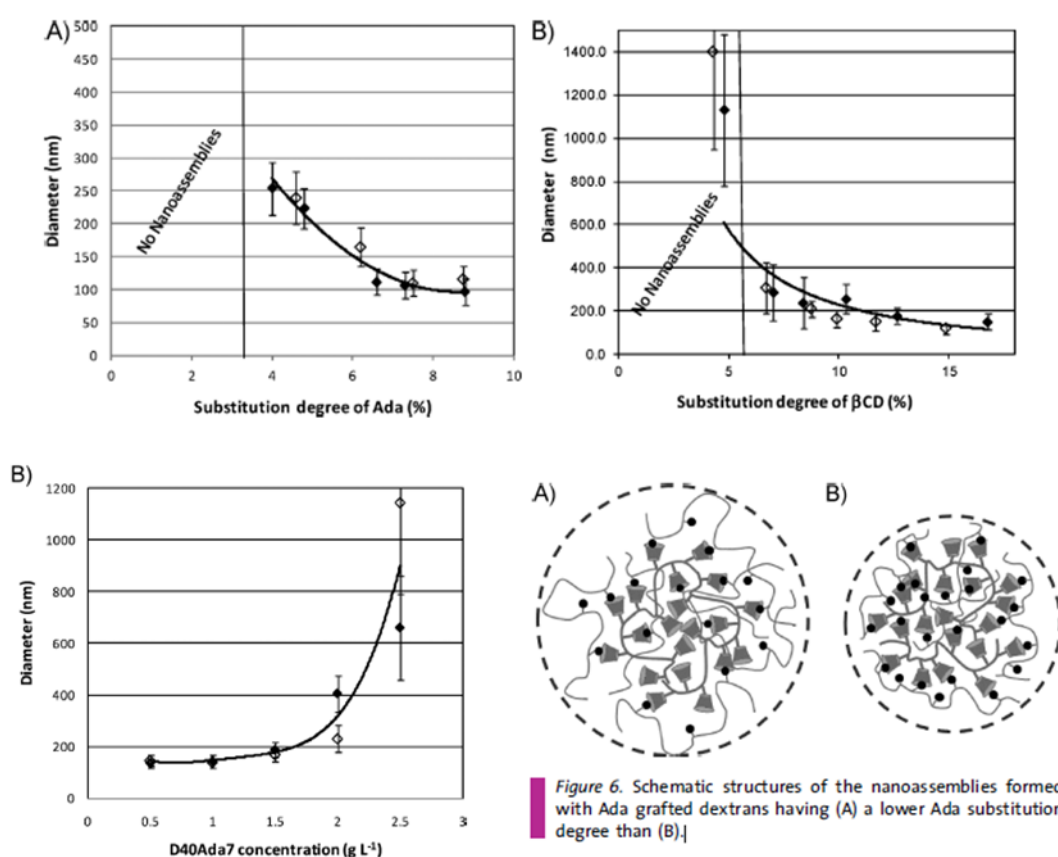
Figure 1.6. Effect of substitution degree, polymer concentration and adamantane to βCD ratio on the sizes of nanogels [34].

Amiel and coworkers have done extensive research on self-assembled nanogels containing βCD and guest moieties, using polymers with βCDs comprising the backbone [35,36], and polymers with βCDs as pendant groups [37,38], and studied their drug loading ability [39,40]. In this study, the nanogels formed spontaneously by βCD- and adamantane-

modified dextrans in aqueous media were investigated. It was found that the association constant for polymer-polymer systems were 30 times higher than adamantane polymer-free βCD systems due to cooperative binding. The size of these nanogels are tunable by changing the grafting ratio of βCD and adamantane, total polymer concentration and adamantane to βCD ratio. There is a threshold substitution degree of both βCD- and adamantane-modified dextrans below which nanogels did not form. The sizes of the nanogels increased with increasing polymer concentration until micro-scale nanogels were formed. Adamantane to βCD ratio, however, is inversely proportional to size. At low ratios, the sizes are larger due to loose network formation while at 1:1 ratio the size is minimized as a tighter network is formed. (Figure 1.6) [34]. The ease of tunability of size and architecture of these nanogels make them a versatile platform for biomedical applications. However, for a more robust delivery platform, additional factors, such as stimuli-responsiveness and active targeting, must also be considered.
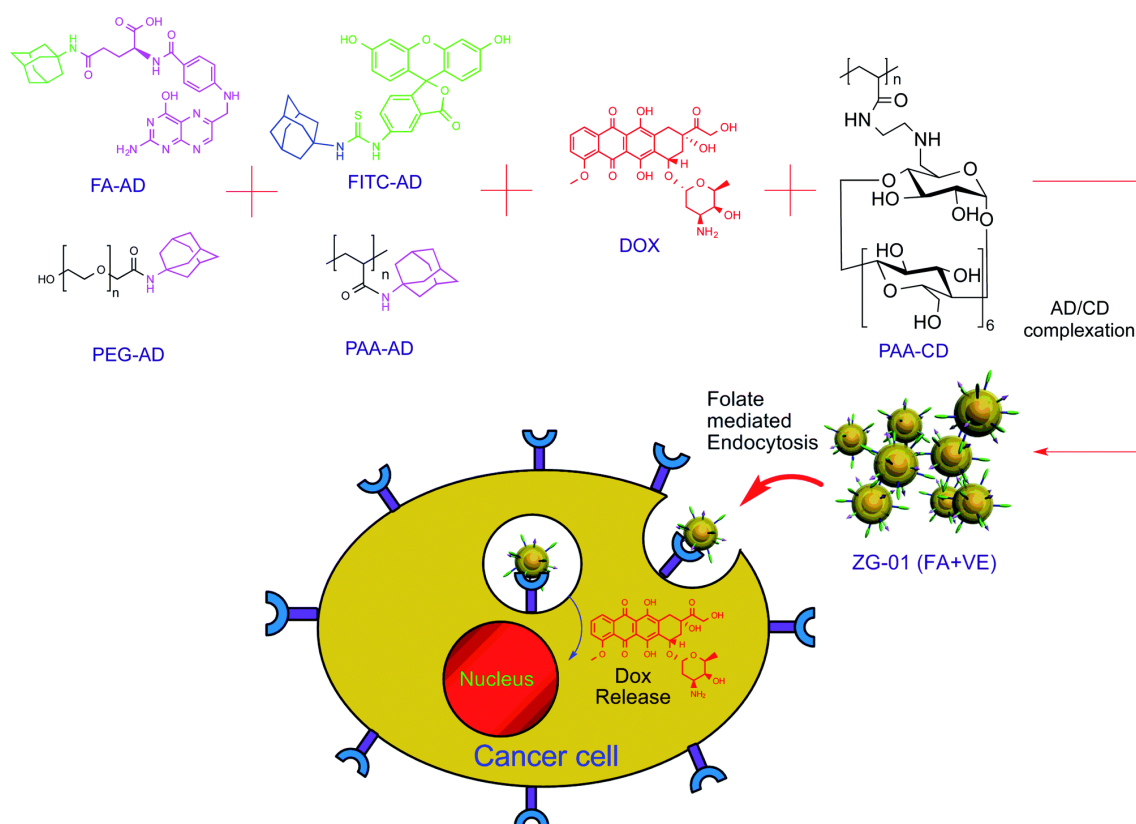
Figure 1.7. Schematic representation of nanocarriers through supramolecular self-assembly for target-specific drug delivery [41].

Zhao and coworkers produced polyacrylate (PAA)-based supramolecular nanoparticles for targeted drug delivery for cancer therapy. The nanoparticles consisted of multiple components: βCD-modified PAA, adamantane-modified PAA, adamantane-modified PEG, adamantane-conjugated fluorescin isothiocyanate for fluoresecent tracing, adamantane-modified folic acid as targeting group and free doxorubicin. (Figure 1.7) The nanoparticles were prepared by sonication method with DMSO and were 35 nm in size which is suitable for good blood circulation. Drug loaded nanoparticles showed significant cytotoxicity while empty nanoparticles were not cytotoxic. Presence of folic acid targeting group made the nanoparticles specific for targeting MDA-MB231 cancer cells but not HEK293 healthy cells. In vivo studies also showed that adding folic acid to nanoparticle structure increases the efficacy of inhibiting tumor growth [41].
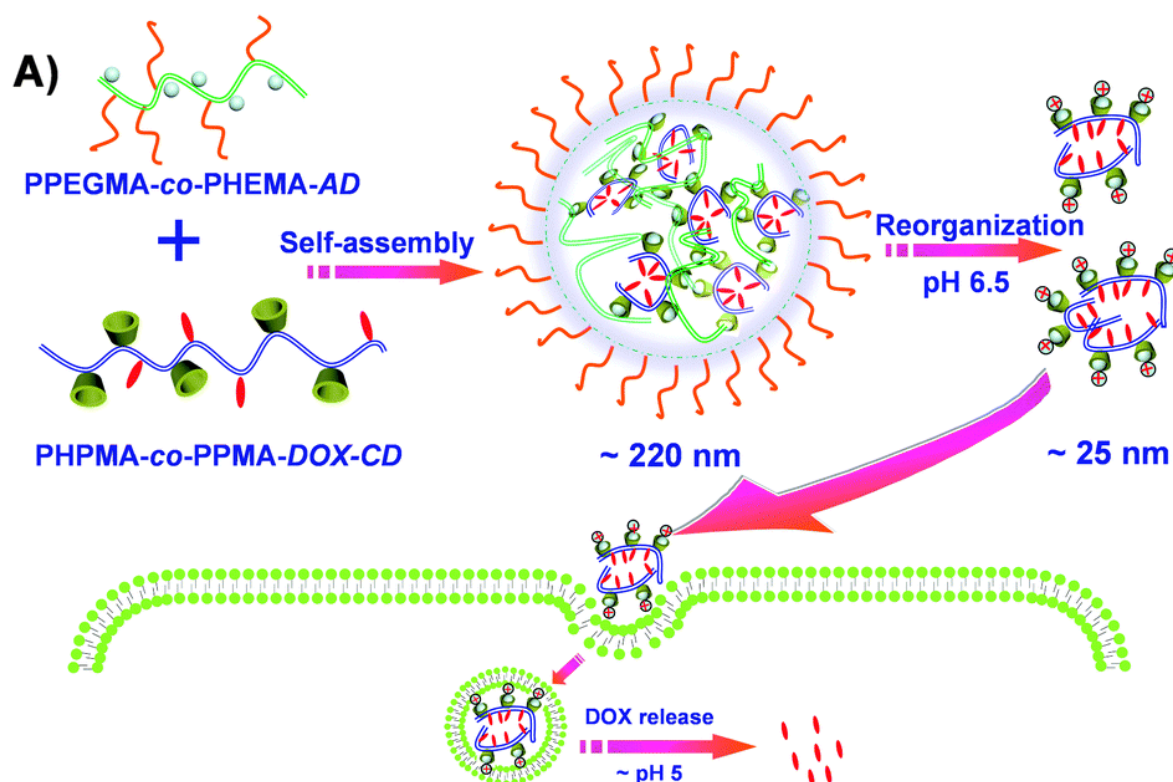
Figure 1.8. Schematic illustration of construction of polymeric nanogels with dual-pH triggered multistage drug delivery [42].

Luo, Ge and coworkers fabricated nanogels based on host-guest interactions between βCD and adamantane, that reorganize into smaller nanogels at pH 6.5, which is the pH of tumor tissue. The smaller gels have improved penetration into the dense tumor tissue matrix.

When gels are internalized by endocytosis, at pH 5.3, they release their cargo, which is doxorubicin. (Figure 1.8) The nanogel is composed of two polymers: a random copolymer of poly(polyethyleneglycol monomethyl ether methacrylate) and adamantane benzoic imine conjugated poly(hydroxyethyl methactrylate) and a random copolymer of poly(N-2-hydroxypropyl methacrylamide) and doxorubicin-hydrazone and βCD conjugated poly(3-azidopropyl methacrylate), done via RAFT. The nanogels were produced by dialysis method with DMSO as solvent and size at neutral pH was 220 nm. At pH 6.5, the benzoic imine bond between polymer backbone and adamantane is cleaved and the doxorubicin and βCD containing copolymer reorganizes into smaller nanogels of size 25 nm. Release studies showed that highest release of doxorubicin was observed at pH 5.3 (endosomal pH), where the hydrazone bond between doxorubicin and polymer backbone is cleaved [42].
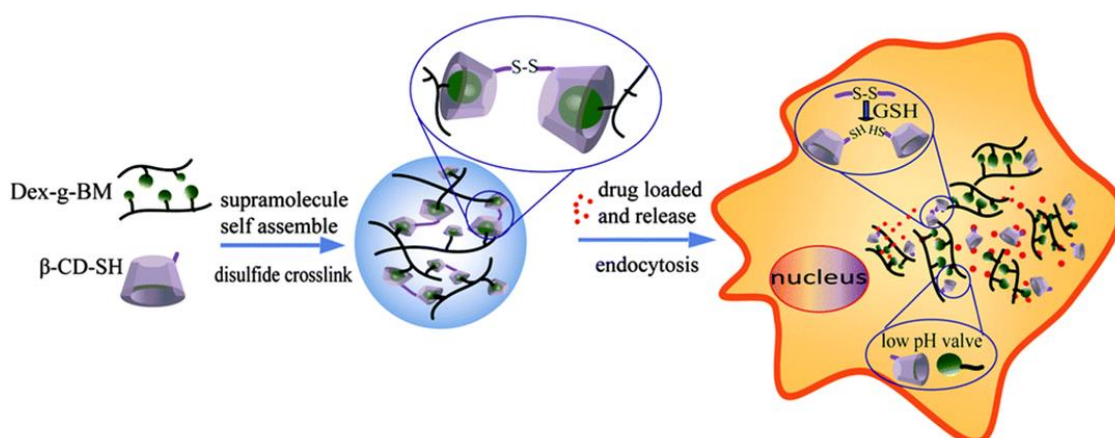
Figure 1.9. Schematic illustration of DOX loading and intracellular microenvironment triggered release from DOX-loaded dual responsive supramolecular nanogels [43].

Besides adamantane, a range of hydrophobic molecules were investigated as guests to form inclusion complexes with βCD. Chen and coworkers designed a nanogel that is sensitive to both the acidic pH and higher glutathione concentration in tumor tissue, using benzylimidazole grafted dextran and disulfide containing bis-βCD linker formed in situ from oxidation of thiol containing βCD. Benzylimidazole forms an inclusion complex with βCD, however, dissociation occurs at low pH. As a control, benzoic acid grafted dextran, which is pH-insensitive, was used (Figure 1.9). Nanogels were 136 nm in netural pH. Increasing GSH and decreasing pH have an increasing effect on the size indicating

dissolution of NG structure. DOX was loaded into the NGs by dialysis method (drug loading was on average 5 w%) and release profiles were investigated at a number of different conditions, summarized in Figure 1.10. As can be seen, while both pH- and GSH-responsiveness contribute to release profile, pH has a markedly higher effect on release [43].
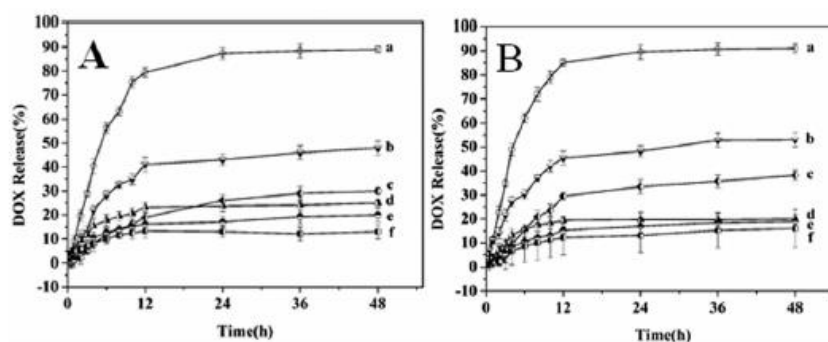
Figure 1.10. In vitro DOX release from NGs at pH 5.3 (a), 6.8 (b), and 7.4 (c), and control NGs at pH 5.3 (d), 6.8 (e), and 7.4 (f) at 37°C in PBS (A: without GSH, B: with GSH) [43].

1.4. Click Chemistry

Click chemistry is the name given to reactions that fit into the bounds of certain criteria. Namely, reactions that are modular, wide in scope, give very high yields, generate only inoffensive byproducts, and are stereospecific. Reactions must also have simple reaction conditions, readily available starting materials and reagents, the use of no solvent or a solvent that is benign or easily removed, and simple product isolation. Some types of "click" reactions are as follows: Nucleophilic opening of highly strained rings such as epoxides, aziridines, cyclic sulfates, cyclic sulfamidates and aziridinium ions, Protecting group reactions such as acetals, ketals and their aza-analogs. Cycloaddition reactions such as Diels-Alder [4+2] and Copper catalyzed Huisgen [3+2] or Huisgen 1,3 dipolar cycloadditon reactions [44].

1.4.1. Copper Catalyzed Huisgen [3+2] Cycloaddition

The thermal cycloaddition of terminal or internal alkynes with organic azides has been known for more than a century. This reaction usually requires prolonged heating and

results in low yields due to the high activation energy barrier and a mixture of 1,4- and 1,5-regioisomers. (Figure 1.11A) In contrast copper catalyzed alkyne azide cycloaddition (CuAAC) (Figure 1.11B), reported first by Sharpless [45] and Meldal [46] in 2002, is regiospecific and has a 10^7–fold increased rate relative to the thermal process, which makes it fast at and below room temperature. The reaction is not significantly affected by the steric and electronic properties of the groups attached to the azide and alkyne centers. It can take place in many protic and aprotic solvents, including water, and is orthogonal to most organic and inorganic functional groups. The 1,2,3-triazole heterocycle product has high chemical stability which allows it to interact with biological molecules, organic and inorganic surfaces and materials. The catalyst can be introduced as Cu (I) salt (CuI or CuBr) or generated in situ by reduction of Cu (II) salts ($CuSO_4$) and an amine containing base such as 2,6-lutidine, triethylamine, pyridine and PMDETA as ligand. Most commonly used catalyst systems are $CuSO_4$/NaAsc and CuBr/PMDETA [47].

Figure 1.11. Thermal cycloaddition of azides and alkynes (A), CuAAC (B) [47].

Due to its aforementioned characteristics, CuAAC is viewed as ideal for chemical synthesis, drug discovery, bioconjugation and biochemistry and is used widely in drug delivery, tissue engineering and other biomedical applications.

2. AIM OF THE STUDY

The aim of this study is to produce self-assembled biodegradable nanogels using host-guest interactions between βCD and adamantane that can be used as drug delivery agents. Bioreductive disulfide bonds were added to the structure to take advantage of increased concentration of GSH in tumor tissue and control the release of cargo (Figure 2.1). βCD-grafted dextran and disulfide containing bis-adamantane linkers were used as building blocks for the nanogel. Dextran, a polysaccharide, was chosen as the backbone due to its high biodegradebility. βCD was attached to dextran by copper catalyzed Huisgen [3+2] cycloaddition ("click" reaction) due to its high efficiency and good yield. Nanogels were formed simply by mixing the βCD functionalized dextran and bis-adamantane together in water. The size and stability of the nanogels are tunable by changing the polymer concentration and βCD to adamantane ratio. The dissolution of the nanogels with reducing agent was studied by addition of DTT and GSH. The optimal combination of linker structure, polymer concentration and βCD to adamantane ratio was determined to continue on with drug loading studies. Doxorubicin (DOX) was chosen as a model drug. DOX was loaded into the nanogels by simple mixing method and dialysis method to compare the drug loading contents and loading efficiencies of the two approaches.
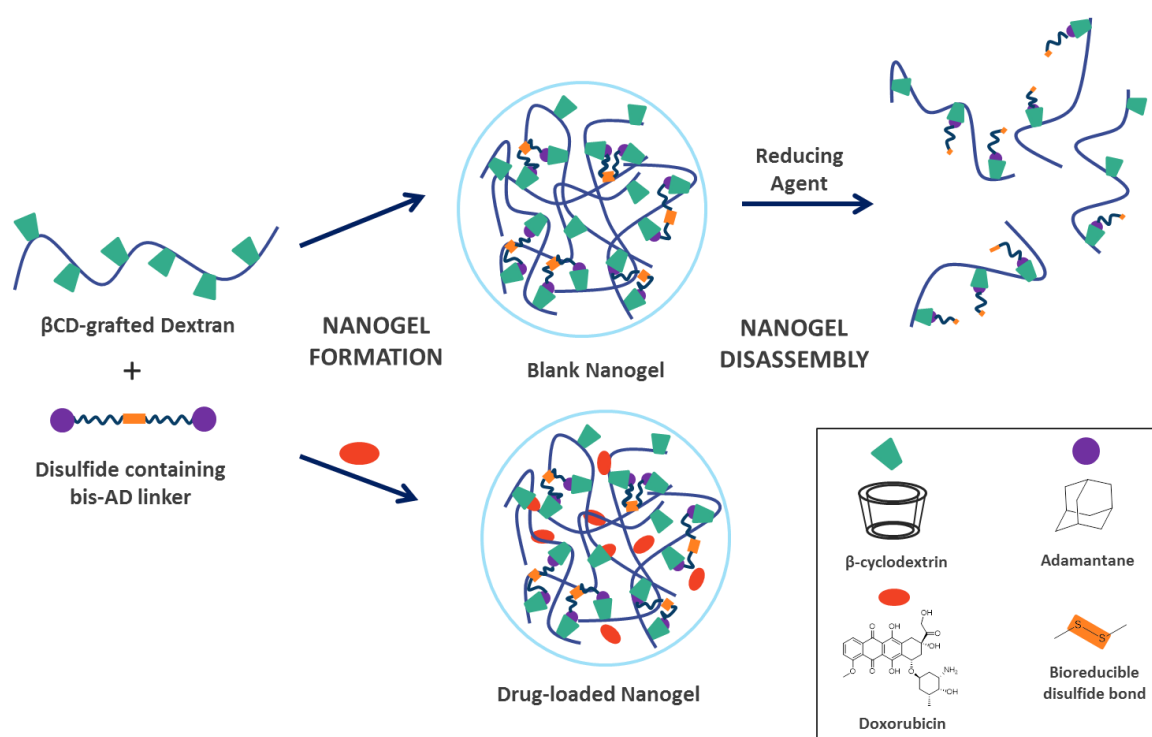
Figure 2.1. General scheme of the project.

3. RESULTS AND DISCUSSION

3.1. First Generation Nanogels

Nanogels were prepared using biodegradable β-cyclodextrin functionalized dextran (DT40-βCD) and bioreducible bis-adamantane linkers containing disulfide bonds. Dextran was chosen as a backbone because it is a polysaccharide and therefore easily degraded in the body with the help of enzymes. Similarly, βCD is an oligosaccharide and is biodegradable. Adamantane is chosen as a guest molecule for βCD because of their high binding affinity (1500 M^{-1}) [25]. The disulfide bond in the linker makes the NG structure sensitive to the presence of bioreducing agents, such as glutathione (GSH) which is found at elevated levels in tumor tissues [48].

3.1.1. βCD Functionalized Dextran

βCD was attached to dextran backbone using Huisgen type 'click' chemistry. For this, alkyne functionalized dextran (DT40-penty-4-oate) and azide bearing βCD (N$_3$βCD) were synthesized. The general route for synthesizing βCD functionalized dextran (DT40-βCD) is shown in Figure 3.1.
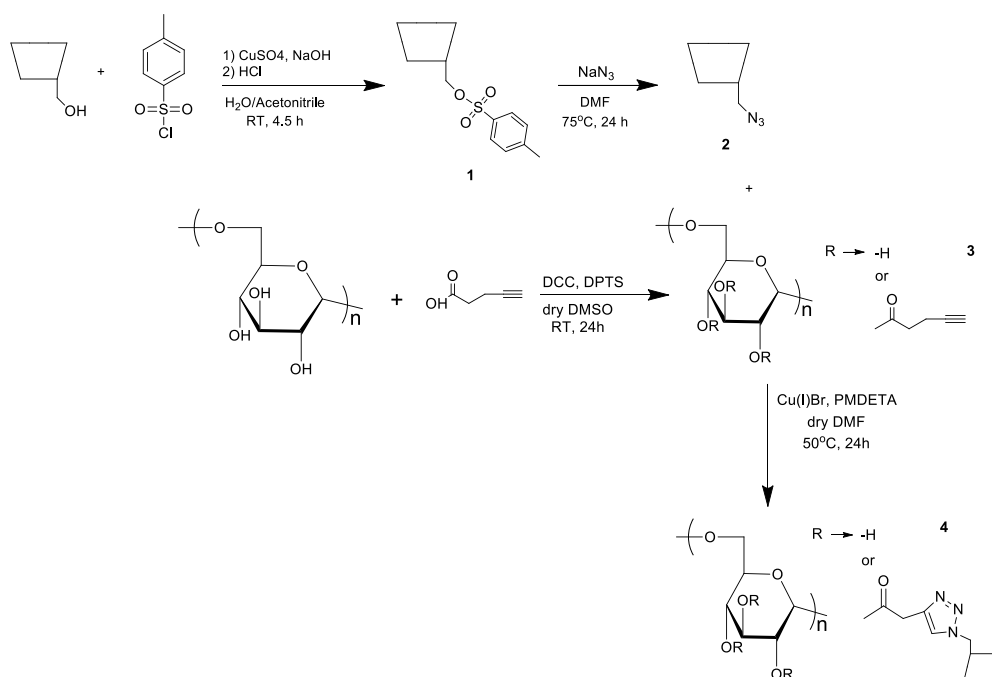
Figure 3.1. Synthetic route for DT40- βCD.

6-Monodeoxy-6-monoazido-βCD (N$_3$βCD) was prepared from 6-O-monotosyl-βCD (TsOβCD) **1**. [49] TsOβCD was synthesized according to literature [50]. Even though the yield was low (31%), use of copper as a catalyst minimized the amount of 6-O-ditosyl-βCD in the product. Purity of the product was monitored by melting point measurement. Melting point was 165°C, which is consistent with literature [51]. Conversion of TsOβCD to N$_3$βCD **2** occurred with high yield (92%). Purity of the product was monitored by the appearance of N$_3$βCD peak (2104 cm^{-1}) and disappearance of residual NaN$_3$ peak (2138 cm^{-1}) in FT-IR (Figure 3.2.).
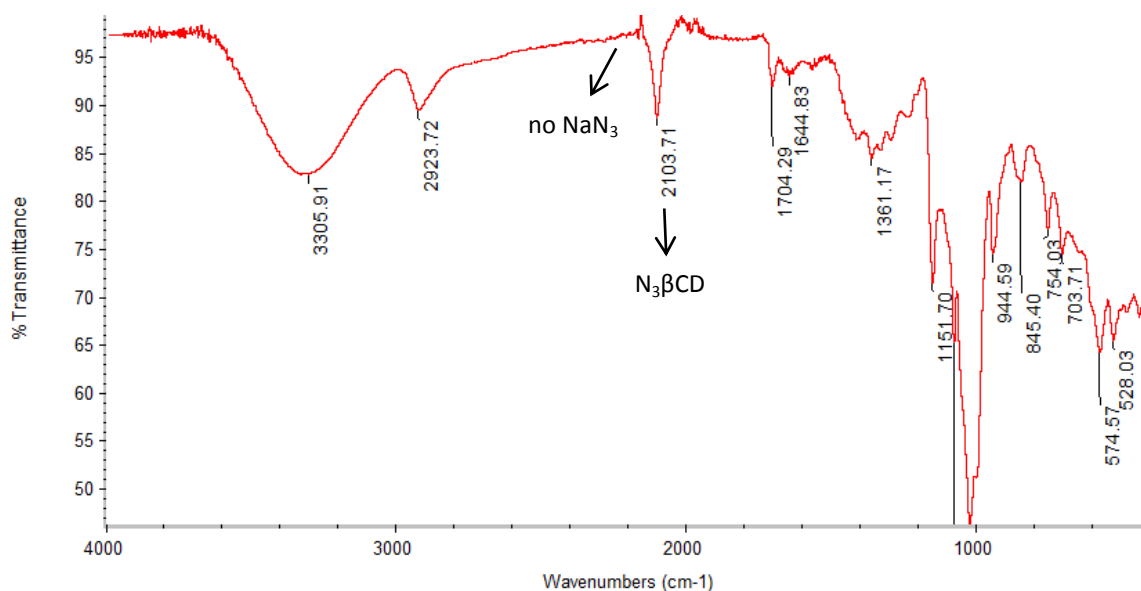
Figure 3.2. FT-IR spectrum of N$_3$βCD.

DT40-penty-4-oates **3** were prepared by DCC coupling of DT40 (Dextran, MW = 40kDa) and 4-pentynoic acid with DPTS as a catalyst using a method modified from literature [52]. Different percentages of functionalization was achieved by varying the amount of 4-pentynoic acid used. Percent functionalization is defined as the amount of alkyne units per 100 anhydroglucose (AHG) units in the backbone. Namely, the ratio of the integral of the terminal alkyne proton (z, 2.77 ppm) and the anomeric proton of the glucose ring (a, 4.83 ppm) determined from ^{1}H-NMR analysis in dDMSO (Figure 3.3).
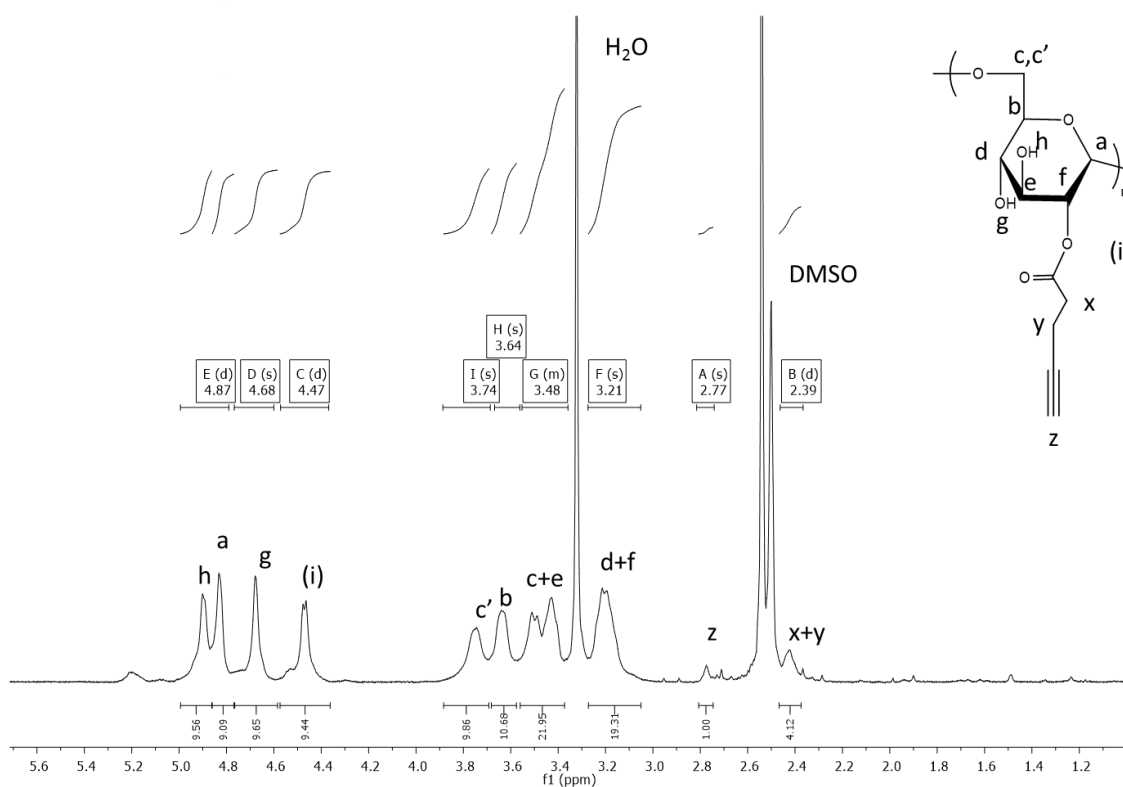
Figure 3.3. ^{1}H-NMR spectrum of DT40-penty-4-oate (10%) in dDMSO.

Alkyne groups are assumed to be randomly distributed along the backbone. It is also assumed that alkyne functionalization has negligible effect on the molecular weight of the polymer [49]. Different percentages of functionalized DT40-penty-4-oates were prepared and used to synthesize the corresponding DT40-βCDs (Table 3.1).

Table 3.1. Synthesis of DT40-penty-4-oates with different functionalization percentages.

| AHG units | Alkyne | % Functionalization | | Yield |
		Theo.	Actual	
1	0.20	10	12±3	86±9%
1	0.30	15	17	89%
1	0.50	25	20	61%
1	0.60	30	20	89%

DT40-βCDs **4** were prepared by copper(I)-catalyzed azide-alkyne cycloaddition (Huisgen type "click" reaction) of DT40-penty-4-oate and N$_3$βCD using Cu(I)Br/PMDETA as the catalyst system [53]. Reaction was carried out at 50°C for 24

hours to overcome the steric hindrance caused by βCDs attached to the backbone. Product was purified by dialysis (MWCO 10K) and any remaining unreacted $N_3βCD$ was monitored by FT-IR (Figure 3.4).
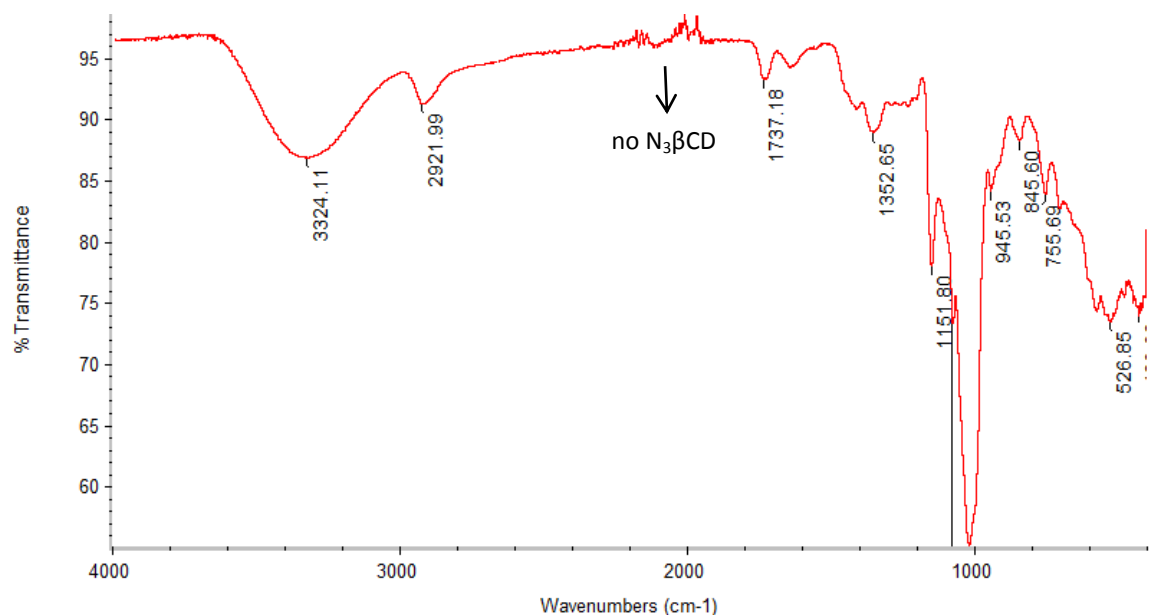
Figure 3.4. FT-IR spectrum of DT40-βCD.

Similar to their alkyne counterparts, the percent functionalization of DT40-βCD was defined as the amount of βCD moiety per 100 AHG units in the backbone. Namely, the ratio of of the triazole proton (a, 7.81 ppm) and the anomeric proton of the glucose ring (b, 4.83 ppm) determined from ^{1}H-NMR analysis in dDMSO. ^{1}H-NMR spectrum also shows the disappearance of the terminal alkyne proton at 2.77 ppm, suggesting no remaining unreacted alkyne units. (Figure 3.5).
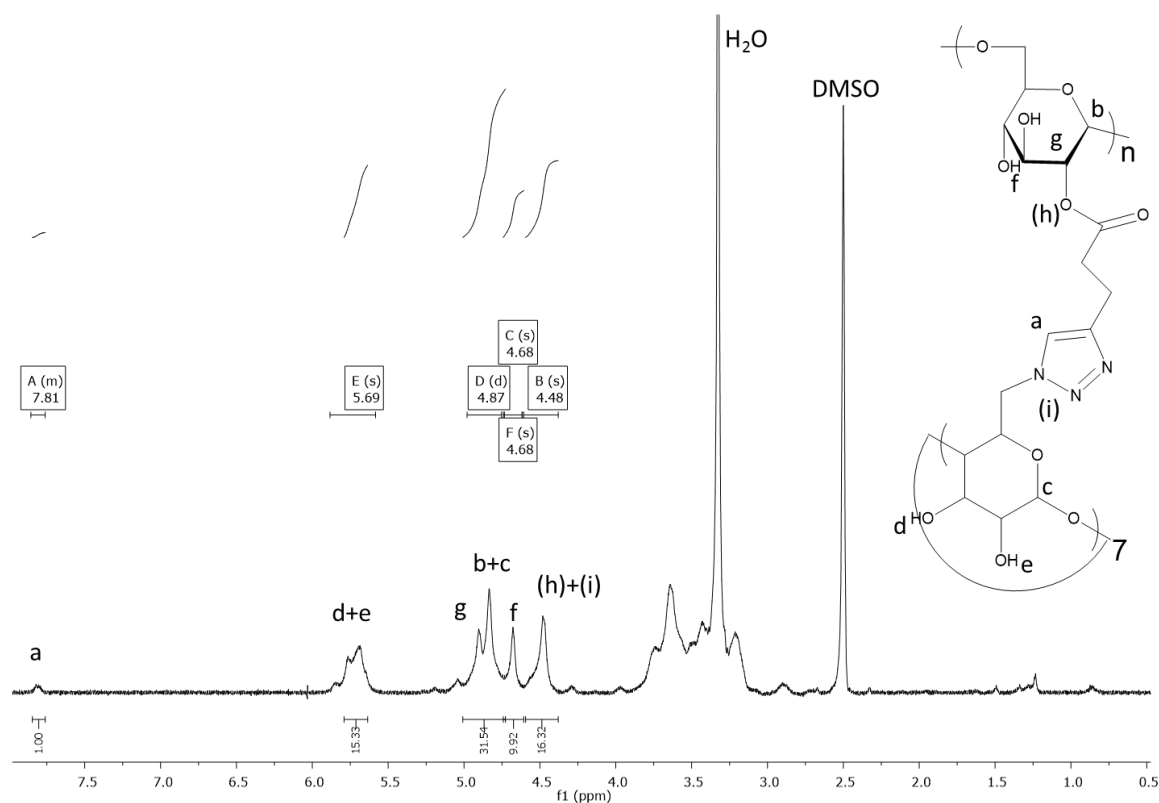
Figure 3.5. ^{1}H-NMR spectrum of DT40-βCD (10%) in dDMSO.

Synthesized DT40-βCDs can be grouped into two categories: 10% and 20% functionalized which can be seen on Table 3.2. respectively.

Table 3.2. Synthesis of DT40-βCDs with different functionalization percentages.

		% βCD			
% Alkyne	Alkyne:Azide	Theo.	Actual	MW$_{theo}$ (kDa)	Yield
12±3	1:4	12±3	10.3±2	66.4±4.4	62±15%
20	1:4	20	20	90.8	50%

3.1.2. Disulfide Containing Bis-Adamantane Linker

Bioreducible bis-AD linkers were synthesized using EDCI coupling of 4,4-dithiodibutyric acid and 1-adamantane methanol with DMAP as the catalyst. The general route for synthesizing the bis-AD linker is shown in Figure 3.6 and ^{1}H-NMR spectrum in CDCl$_3$ is given in Figure 3.7.
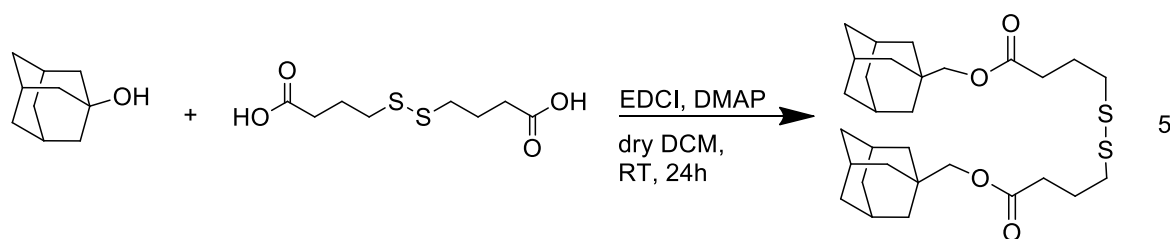
Figure 3.6. Synthetic route for bis-AD linker.
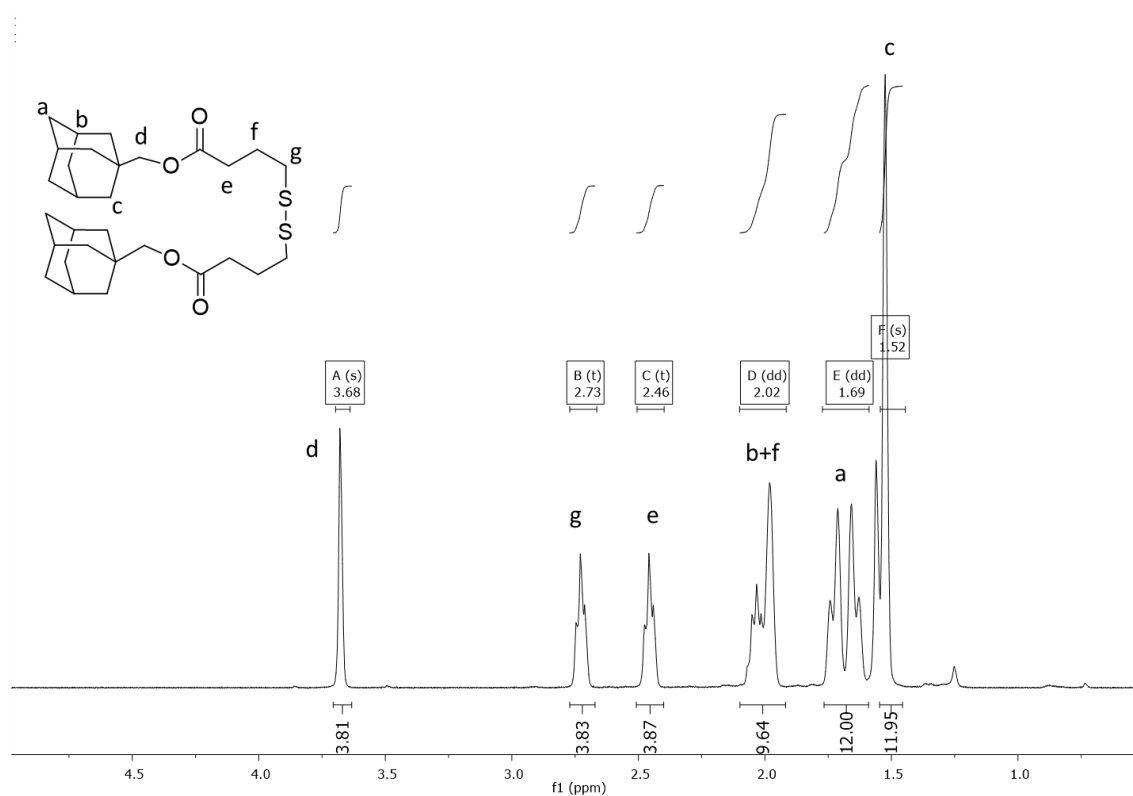
Figure 3.7. ^{1}H-NMR spectrum of bis-AD linker in CDCl$_3$.

3.1.3. Nanogel Preparation

As bis-AD linker was not soluble in water, solvent evaporation method was used to prepare the NGs. Briefly, various concentrations of DT40-βCD polymers in MQ water were prepared and stirred overnight to equilibrate. Solutions were then filtered (pore size 220 nm) before use. Stock solution of bis-AD linker was prepared in MeOH. Volume of stock solution needed to achieve known equivalents of βCD to AD was calculated and added to the polymer solution. The solution was stirred, oncovered, overnight under the

fume hood to allow MeOH to evaporate and for the NGs to equilibrate as can be seen in Figure 3.8. The initial polymer solution is transparent while the NG solution becomes turbid.
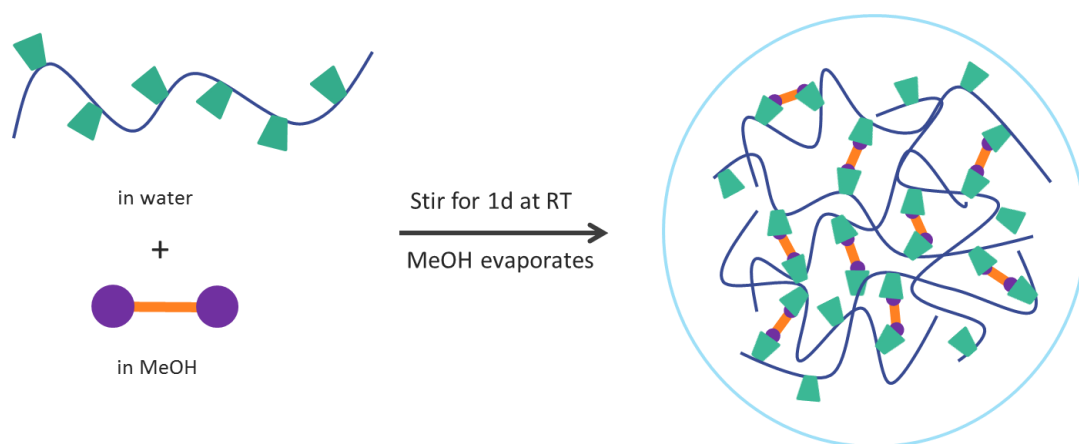
Figure 3.8. General method for first generation nanogels.

The formation of NGs was followed by size measurements using Dynamic Light Scattering (DLS). As a reference, sizes of the polymers were also taken and are listed in Table 3.3. 20% functionalized DT40-βCD has a smaller size than 10% functionalized DT40-βCD which is thought to be due to βCD's tendency for self-aggregation [54].

Table 3.3. Size measurements of parent polymers by DLS.

	Size (nm)	PDI
DT40	7.6±1.9	0.378
DT40-βCD (10%)	8.4±2.2	0.429
DT40-βCD (20%)	7.3±1.8	0.574

A summary of first generation NGs prepared can be found in Table 3.4. As the amount of bis-AD linker used is decreased, the sizes of the NGs increase. The low amount of linker leads to a looser structure that is bigger in size. As the % functionalization of DT40-βCD is increased, the sizes of the NG decrease. The higher amount of available crosslinking sites on the polymer backbone makes the NG structure tighter and smaller in size [34]. PDI values are within an acceptable range (below 0.4).

Table 3.4. Size measurements of first generation NGs (C_p 1 mg/mL).

% βCD	bis-AD linker (eq)	Size (nm)	PDI
10	0.75	163±53	0.493
10	1	129±62	0.362
20	1	95±43	0.171

3.1.4. Nanogel Disassembly with Reducing Agent

After the preparation of NGs, their responsiveness to reducing agents was investigated. To acheive this, DTT was added to NG solutions and the sizes were monitored by DLS over a time period. For this study, NGs made with DT40-βCD (10%) with a polymer concentration of 1 mg/mL were chosen.
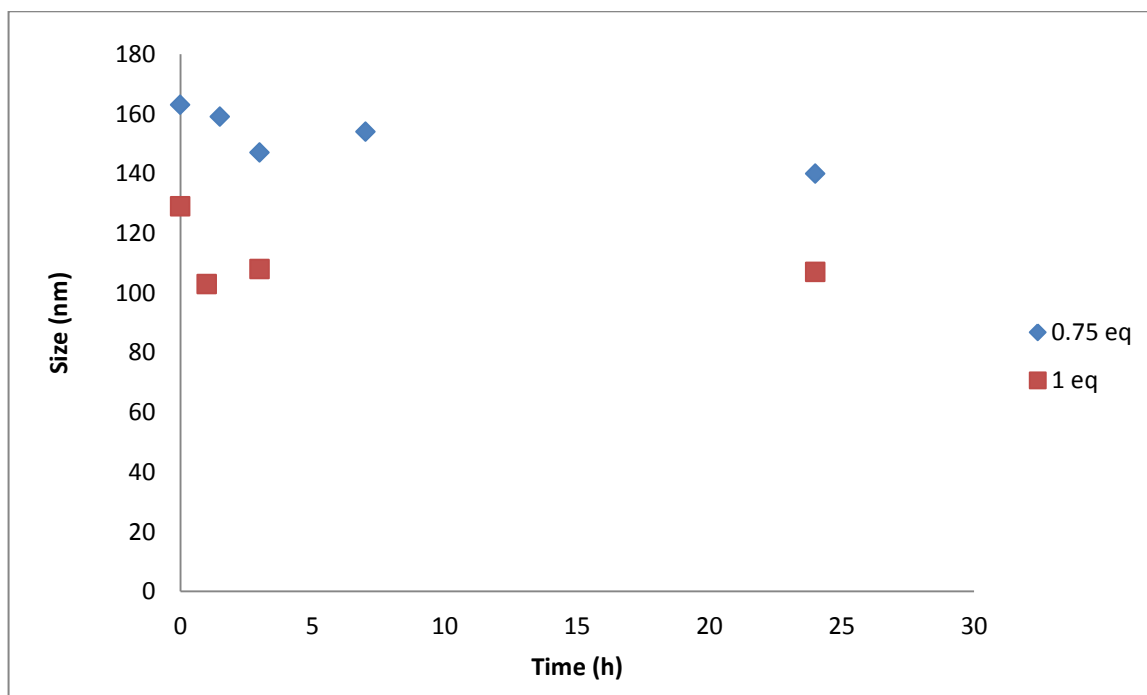
Figure 3.9. Disassembly of first generation NGs made with DT40-βCD (10%) (C_p 1 mg/mL) with 15 mM DTT.

As can be seen in Figure 3.9, the sizes of NGs remained constant over 24 hours, meaning first generation NGs were unresponsive to reducing agent DTT. This is thought to be due to the local hydrophibicity and steric hindrance cause by βCD around the disulfide

bond that prevents DTT from reaching it. To overcome this, the structre of the linker was changed to prepare second generation NGs.

3.2. Second Generation Nanogels

For the second generation NGs, a tetraethyleneglycol (TEG) spacer was added to the linker between AD and disulfide moieties to increase local hydrophilicity and overcome the steric hindrance.

3.2.1. Disulfide Containing Bis-Adamantane-TEG Linker

Bioreducible bis-AD-TEG linkers were synthesized using EDCI coupling of 4,4-dithiodibutyric acid and adamantane-TEG-OH with DMAP as the catalyst. The general route for synthesizing the bis-AD-TEG linker is shown in Figure 3.10. and ^{1}H-NMR spectrum of final product is given in Figure 3.11.
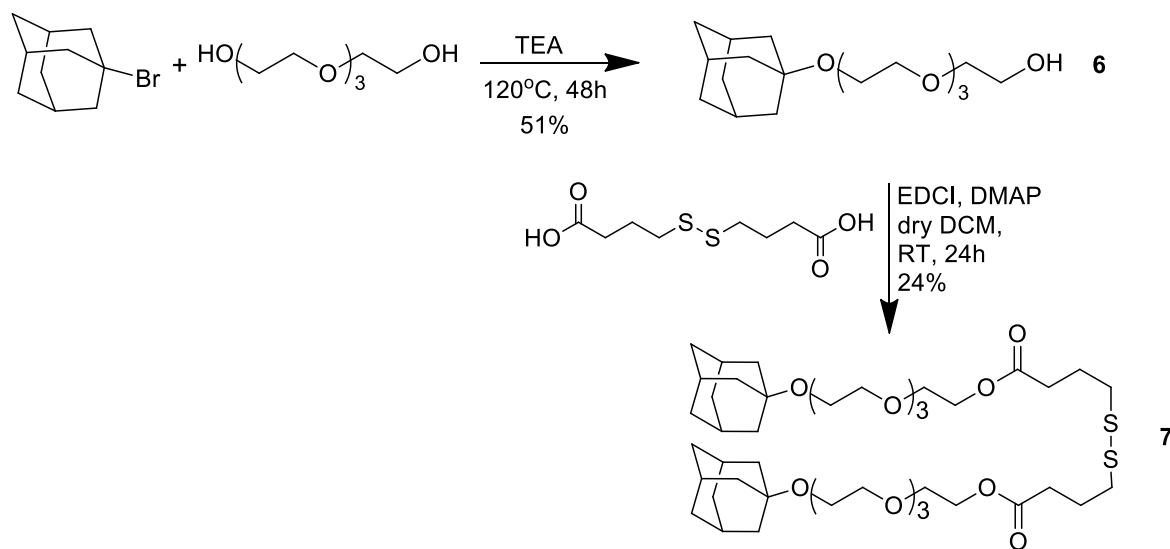

Figure 3.10. Synthetic route for AD-TEG-OH **6** and bis-AD-TEG linker **7**.
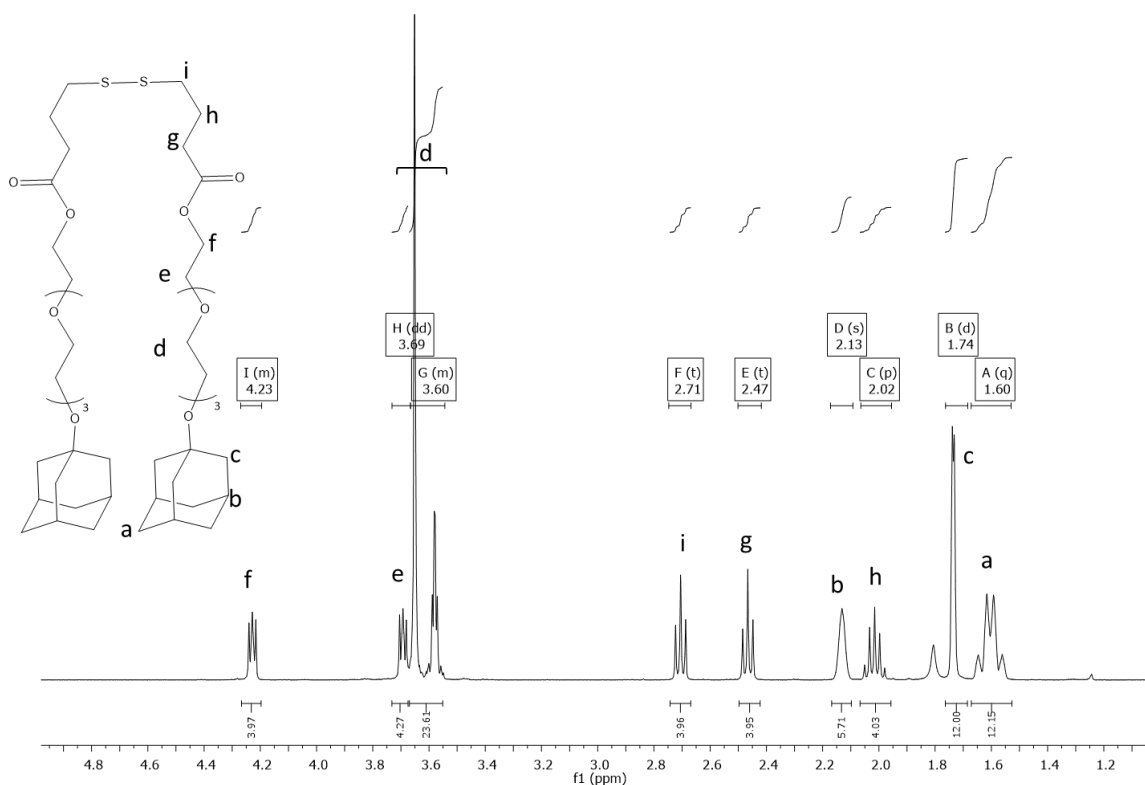
Figure 3.11. ^{1}H-NMR spectrum of bis-AD-TEG linker in CDCl₃.

3.2.2. Nanogel Preparation

Since the bis-AD-TEG linker was soluble in water, NGs were formed by simple mixing. Briefly, various concentrations of DT40-βCD polymers in MQ water and stock solution of bis-AD-TEG linker were prepared in MeOH as described previously. Volume of solution needed to achieve known equivalents of βCD to AD was calculated, added to a vial and MeOH was evaporated under vacuum. The polymer solution was added the the same vial and stirred overnight at RT for the NGs to equilibrate as can be seen in Figure 3.12. Similar to first generation NGs, polymer solution is transparent while the NG solution becomes turbid.
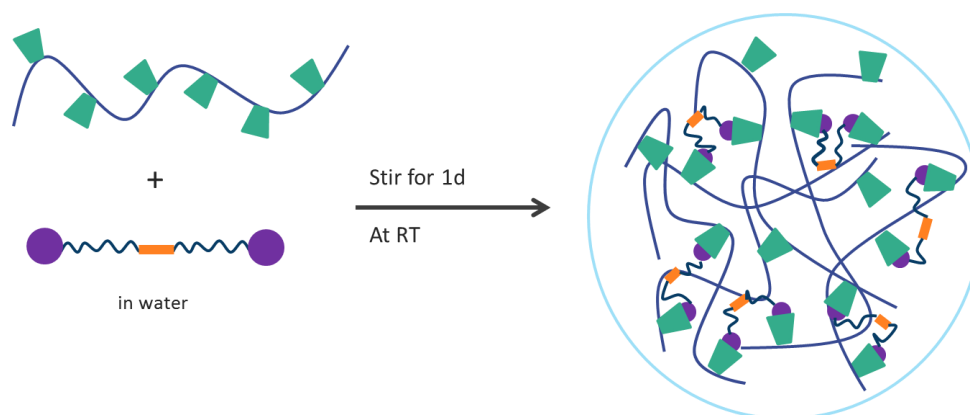
Figure 3.12. General method for second generation nanogels.

A summary of second generation NGs prepared can be found in Table 3.5. Sizes are, in general, below 200 nm which makes the NGs suitable for drug delivery applications. PDI values are between 0.2-0.4 which is an acceptable range. In accordance with results from first generation NGs, NGs made with DT40-βCD (20%) in general have a smaller size than those made with DT40-βCD (10%).

Table 3.5. Size measurements of second generation NGs.

NG #	% βCD	C_p (mg/mL)	bis-AD-TEG linker (eq)	Size (nm)	PDI
1	10	1	0.5	7.3±1.8	0.355
2	10	1	0.75	159±87	0.255
3	10	1	1	146±74	0.208
4	10	1.5	0.75	160±56	0.502
5	10	1.5	1	174±87	0.243
6	10	3	0.75	235±127	0.225
7	10	3	1	247±162	0.290
8	20	1	0.25	7.1±1.8	0.614
9	20	1	0.5	97±51	0.297
10	20	1	0.88	84±36	0.239
11	20	1	1	165±77	0.140

Polymer concentration and amount of linker also play a key role in determining NG size. From Figure 3.13, it can be seen that size increases with increasing polymer concentration. Decreasing the amount of bis-AD-TEG linker used makes a loosely held together gel and so increases the size in accordance with previous results. Also, a threshold βCD-AD equivalence exists between 0.5 and 0.75, below which no NG formation is

observed. This value is lower (between 0.25-0.50) for NGs made with DT40-βCD (20%) due to the higher number of βCD cavities available for crosslinking on polymer backbone.
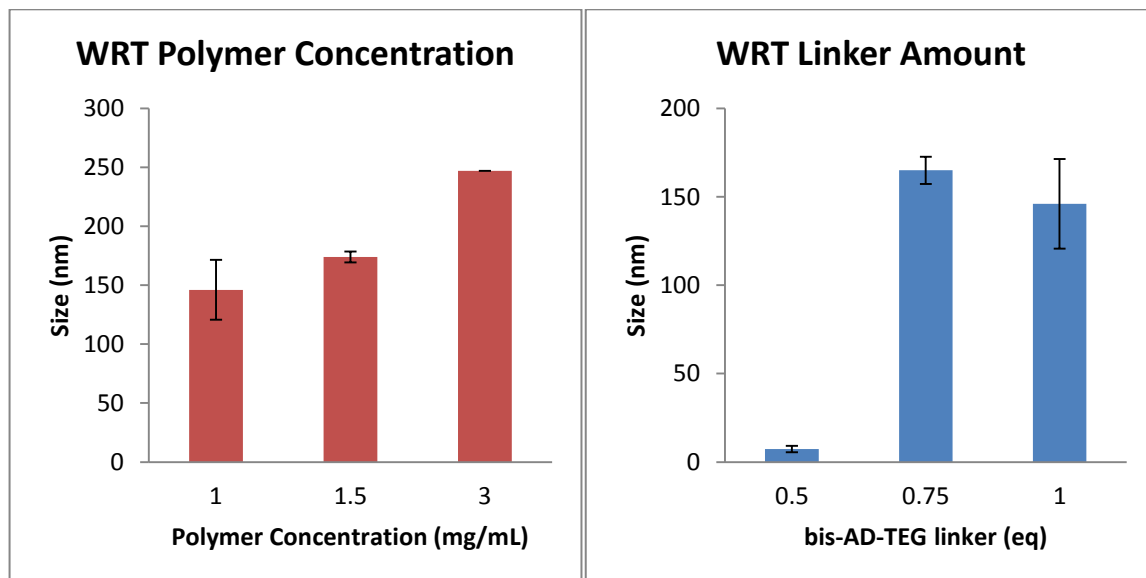
Figure 3.13. Trends in NG size (DT40-βCD 10%) with respect to polymer concentration (bis-AD-TEG linker 1 eq) and bis-AD-TEG linker amount (C_p 1 mg/mL).

3.2.3. Nanogel Disassembly with Reducing Agent

After the preparation of NGs, their responsiveness to reducing agents was investigated. To acheive this, DTT and GSH were added to NG solutions and the sizes were monitored by DLS over a time period. This was done at at 37°C to simulate living tissue conditions.

From Figure 3.14, it can be seen that for NGs made with DT40-βCD (10%), addition of DTT causes the size to decrease to around 10 nm within 3 hours which indicates disassembly of nanogel. Addition of GSH, however, causes the size to increase, as can be seen in Figure 3.15. This is reasonable if the method by which disulfide bonds are cleaved by DTT and GSH are considered. From Figure 3.16, it can be seen that while DTT simply cleaves the disulfide bond to produce two thiols, GSH forms a dilsulfide with one of the thiols it produces. Therefore, after addition of GSH, polymer backbone bears moieties that can form hydrogen bonds which causes a larger and looser structure to form.
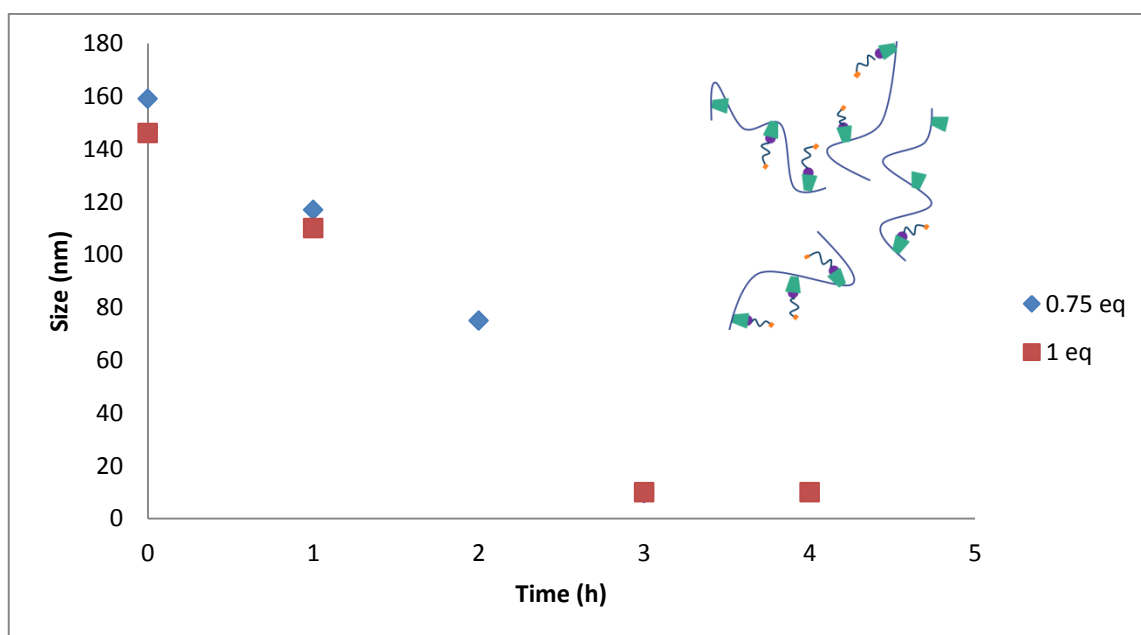
Figure 3.14. Disassembly of second generation NGs with 15 mM DTT at 37°C (DT40-βCD 10%, C_p 1 mg/mL).
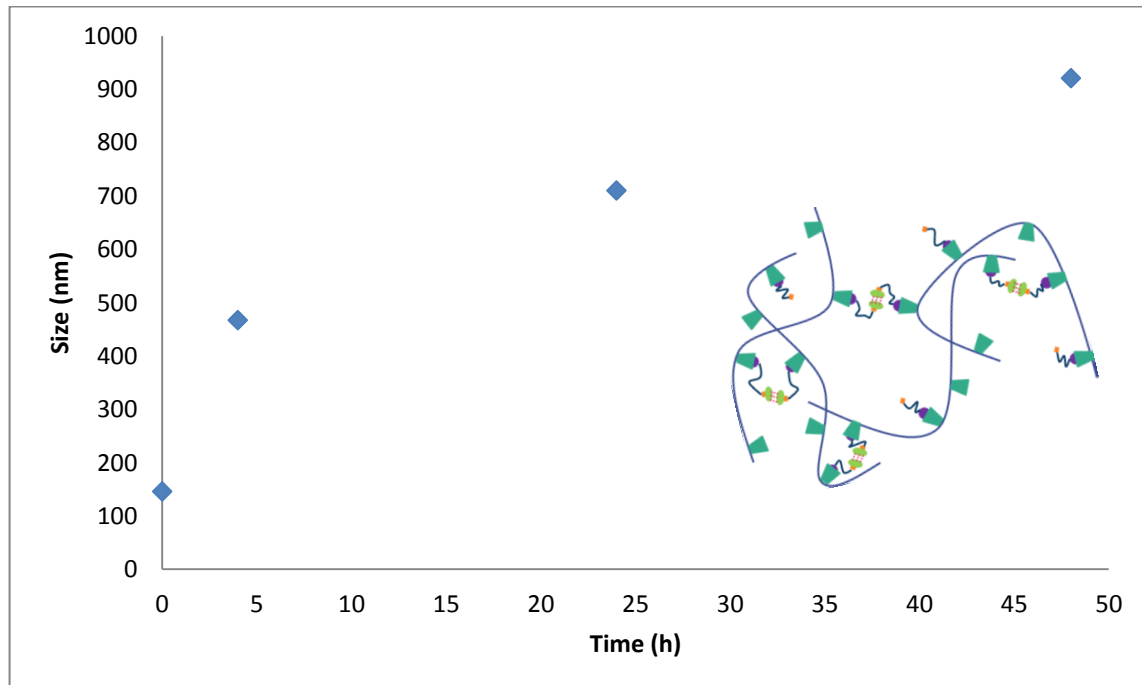
Figure 3.15. Disassembly of second generation NG with 15 mM GSH at 37°C (DT40-βCD 10%, C_p 1 mg/mL, 1 eq bis-AD-TEG linker).
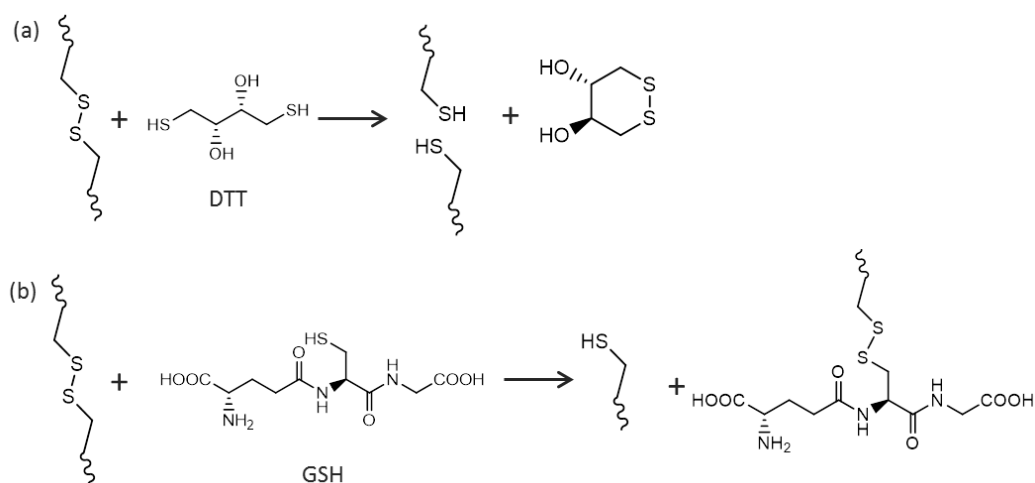
Figure 3.16. Reduction of disulfide bond by DTT (a) and GSH (b).

NGs made by DT40-βCD (20%) on the other hand, are unresponsive to the presence of reducing agents as can be seen from Figure 3.17. This is thought to be due to the thighter structure of the NG that prevents reducing agent to diffuse through the structure to reach the disulfide bonds.
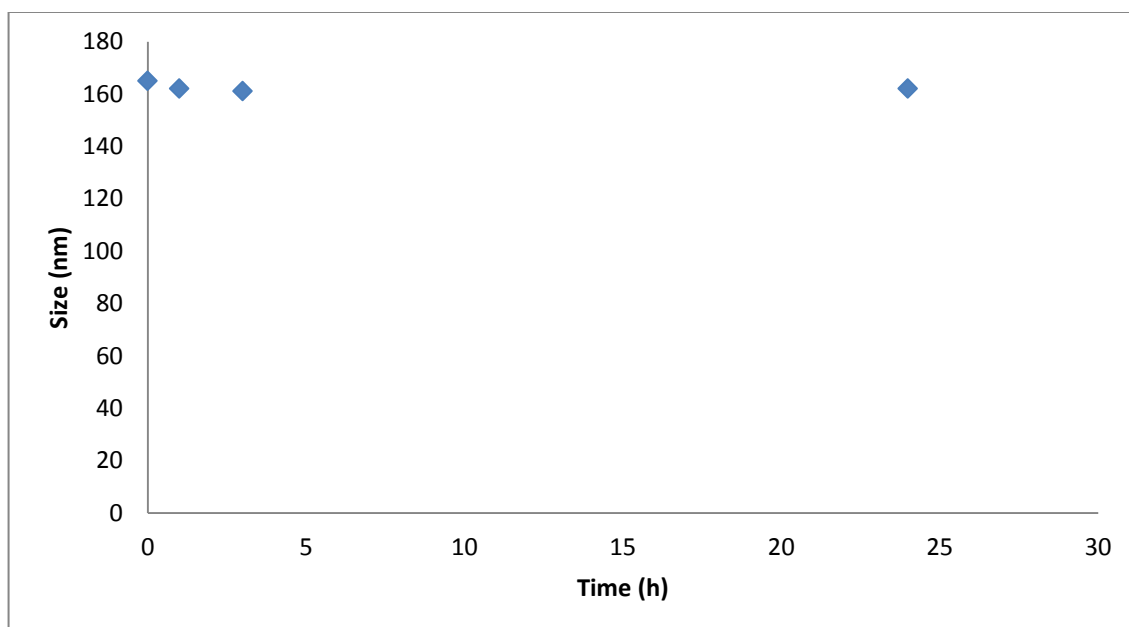
Figure 3.17. Disassembly of second generation NGs with 15 mM DTT at 37°C (DT40-βCD 20%, C$_p$ 1 mg/mL, 1 eq bis-AD-TEG linker).

3.3. Drug Loaded Nanogels

Second generation NGs made with 10% functionalized DT40-βCD were chosen for drug loading experiments as they were responsive to DTT and GSH. Various methods for drug loading were investigated to obtain an optimized procedure. Doxorubicin (DOX) was chosen as a model drug because it can be followed by Fluorescence and UV-Vis spectroscopy and it can also form an inclusion complex with βCD [55].

The first method used was simple mixing. This method is almost identical to the preparation of second generation NGs. DT40-βCD solutions in MQ water were prepared and stirred overnight, the filtered (220 nm). After that three different routes were investigated, which are summarized in Table 3.6. DOX.HCl and bis-AD-TEG linker were added to polymer solution and stirred overnight. However, as can be seen from the table, this method failed to produce NGs in a consistent manner at different polymer concentrations, linker amounts and DOX amounts. The NGs that were produced were cleared of any remaining DOX by dialysis (MWCO 3500, 6h) against MQ water. Drug loading capacities (DL) and loading efficiencies (LE) were determined using UV-Vis Spectrospy based on a previously drawn calibration curve using Equations 4.1 and 4.2 respectively. At the end the sizes of the NGs were too large (>200 nm) even though the control NG prepared without added DOX is of an acceptable size (102 nm). Also the DL and LE values were low.

Table 3.6. Different combinations used to prepare DOX loaded nanogels by mixing method.

| NG # | C_p (mg/mL) | bis-AD-TEG linker (eq) | DOX.HCl (wt %) | Solvent | Sonication | DLS Measurements | | DL (%) | LE (%) |
						Size (nm)	PDI		
1	1	0.75	-	-	+	105±19	0.343	-	-
2	1	0.75	11	-	-	252±140	0.303	1.3	5.7
3	1	0.75	22	-	+	577±147	0.662	2	4.4
4	1	1	11	-	+	348±67	0.832	1.4	12
5	1	-	11	-	-	8.3±1.6	0.507	-	-
6**	1	-	11	-	-	7.7±1.1	0.771	-	-
7	1	1	20	-	-	5.4±1.3	0.617	-	-
8	1.5	0.75	6	-	-	7.9±1.2	0.828	-	-
9	1.5	0.75	15	-	-	10±1.8	0.989	-	-
10	1.5	0.75	20	-	-	7.7±2.3	0.916	-	-
11*	1.5	1	5	MeOH	-	7.5±1.5	0.809	-	-
12	1.5	1	11	-	-	592±112	0.926	0.8	6
13	1.5	1	15	-	-	9.5±1.7	0.985	-	-
14	1.5	1	-	-	-	102±78	0.392	-	-
15*	1.5	1.25	5	MeOH	-	7.4±1.2	0.596	-	-
16*	1.5	1.5	5	MeOH	-	6.9±1.4	0.908	-	-

* DOX precipitated

** DT40 was used

In order to increase drug loading, after the polymer solution was prepared and stirred overnight, DOX.HCl was added to the solution and the mixture was sonicated for 2 hours to facilitate host-guest interactions between DOX and βCD cavity. After, the linker was added and the mixture was stirred overnight. Free DOX was removed by dialysis (MWCO 3500, 6h) against MQ water. As can be seen from Table 3.6, there was no appreciable increase of DL and LE values and the sizes continued to be above 200 nm. As a final method, a route similar to first generation NGs were used. Namely, bis-AD-TEG linker and DOX.HCl were dissolved in minimum amount of MeOH and added to the previously prepared polymer solution and stirred, uncovered, overnight for MeOH to evaporate. However, this method caused DOX to precipitate out of the solution and no NGs were formed.

In search of a more efficient route to prepare DOX loaded NGs, dialysis method was investigated [43]. 5 mg DT40-βCD polymer along with different amounts of bis-AD-TEG linker, DOX.HCl and TEA were dissolved in 1 mL DMSO and stirred overnight. Then DMSO solution was added dropwise to different amounts of MQ water and stirred for 30 minutes. DMSO and free DOX were removed by dialysis (MWCO 3500, 4.5 h) against MQ water. Results for different combinations can bee seen on Table 3.7. It can be seen that the dilution ratio plays an important role in the sizes of the NGs. For low dilution values, the sizes of the NGs are above 400 nm. However when the dilution is increased to 1:15, the sizes drop to 180 nm which is an acceptable value for use in drug delivery applications. DL remains in the 2-3% range regardless of the amount of DOX added to the initial solution. In fact, adding high amounts (>10%) of DOX hinders the formation of NGs by precipitating and causing large agglomerations. In-situ neutralization of DOX.HCl by TEA increases DL and LE values. Amount of linker used also has an effect on NG formation. Most suitable NG was produced using 1 eq bis-AD-TEG linker, 5 wt% DOX and TEA with 1:15 dilution (DLNG) and was chosen to do further studies. The TEM image for DLNG can be seen in Figure 3.18 which confirm their sizes to be below 200 nm.

Table 3.7. Different combinations used to prepare DOX loaded nanogels by dialysis method (C_p 5 mg/mL in DMSO).

| NG # | bis-AD-TEG linker (eq) | DOX.HCl (wt %) | TEA*** | Dilution | DLS Measurements | | | |
					Size (nm)	PDI	DL (%)	LE (%)
1	0.75	20	-	1:5	3501±845	0.468	1.2	6
2	0.75	20	-	1:6	436±190	0.194	1.1	5
3	0.75	20	-	1:9	436±141	0.189	2.7	14
4	0.75	40	-	1:15	220±90	0.211	2	4.9
5	1	5	+	1:15	183±124	0.280	2.4	46
6*	1	8	+	1:15	170±56 (70%), 632±218 (30%)	0.551	3	38
7	1	10	+	1:15	8.3±1.6	0.779	2.5	24
8	1	20	-	1:6	438±154	0.160	1.5	7.5
9*	1	20	-	1:15	175±68	0.115	1.3	6
10*	1	20	+	1:15	3196±752	0.747	2.7	14
11	1	-	-	1:15	131±60	0.127	-	-
12*	2	5	+	1:15	1130±202	0.502	0.8	14
13	-	20	-	1:6	254±56	0.455	2.2	11
14**	-	20	-	1:6	147±24	1.000	1.2	6

* DOX precipitated

** DT40 was used

*** 20 equivalents of TEA to DOX.HCl was used

Figure 3.18. TEM image of DOX loaded nanogel (DLNG).
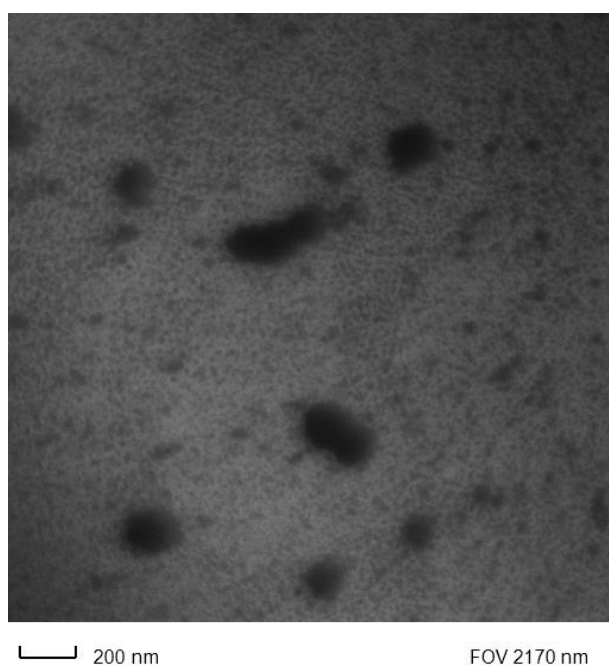
The responsiveness of DLNGs were studied with respect to different DTT concentrations at 37$^{\mathrm{o}}$C. The results are summarized in Figure 3.19. At DTT concentrations 1 mM and 10 mM, the DLNGs were stable over 48 hours, while at 100 mM disassembly ocurred after 11 hours.
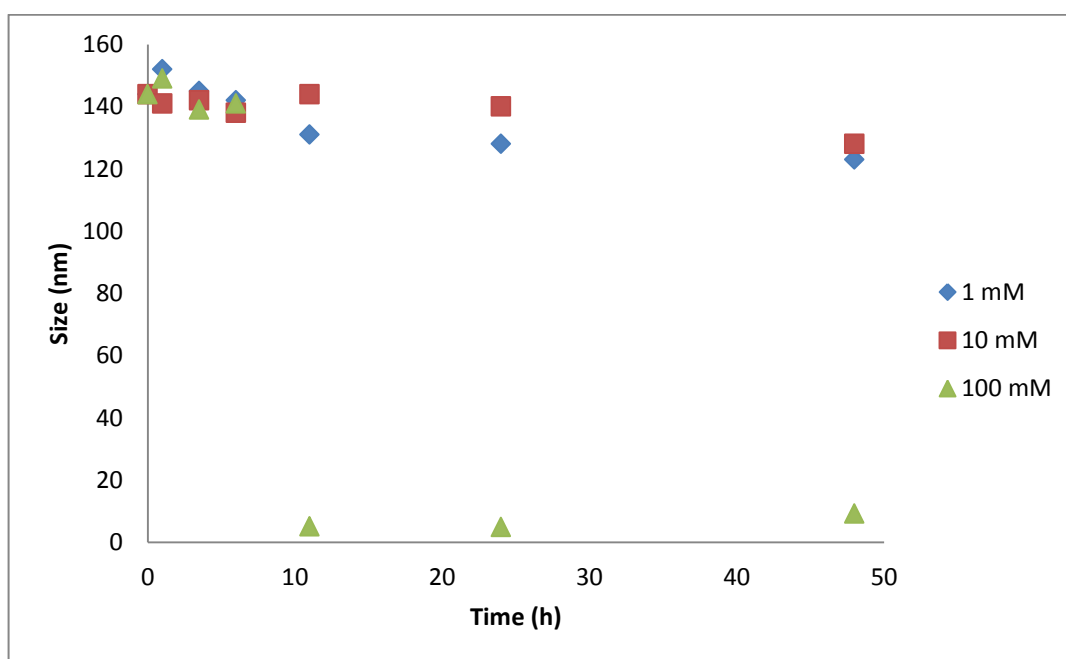
Figure 3.19. Disassembly of DLNGs at different DTT concentrations at 37$^{\mathrm{o}}$C.

4. EXPERIMENTAL

4.1. Materials and Methods

Dextran (DT40, MW 40 kDa) was purchased from Pharmacosmos and dried in vacuo at 80°C overnight prior to use. All reagents were obtained from commercial sources (Merck, Aldrich and Alfa Aesar) and were used as received unless otherwise stated. Dry DCM was obtained from ScimatCo Purification System, other dry solvents were dried over molecular sieves. Characterizations of synthesized componunds were done by ^{1}H-NMR spectroscopy (Varian 400 MHz) and Fourier transform infrared (FT-IR) spectroscopy (Thermo Fisher Scientific Inc. Nicolet 380). Size measurements were taken using Zetasizer Nano particle analyzer series (Malvern), and imaging was done using Transmission Electron Microscopy (TEM, LVEM5 microscope operated at 5 kV). Drug loading content was determined using UV-Vis spectroscopy.

4.2. Synthesis

4.2.1. Synthesis of βCD Functionalized Dextran

<u>4.2.1.1. 6-O-Monotosyl-βCD.</u> This reaction was carried out according to literature [50]. To a solution of βCD (3 g, 2.67 mmol) in 100 mL MQ water, $CuSO_4.5H_2O$ (2 g, 8 mmol) in 200 mL MQ water and NaOH (2.67 g, 40 mmol) in 67 mL MQ water were successively added. In a separate flask, solution of tosyl chloride (4 g, 21 mmol) in 27 mL acetonitrile was prepared. After 10 minutes, tosyl chloride solution was added dropwise to βCD solution over 1 hour. The solution was stirred at RT for 4.5 hours. Then, the solution was neutralized by addition of 13 mL 1 M HCl. The salts were filtered off with sintered glass. From the filtrate, ¾ of the water was evaporated via lyophilization. Crude product was removed by filtration and washed with acetone (2 x 10.5 mL) and ether (2 x 8 mL). Product was then recrystallized in 40 mL water twice. Pure product **1** was obtained as a white solid (1.08 g, 31%).
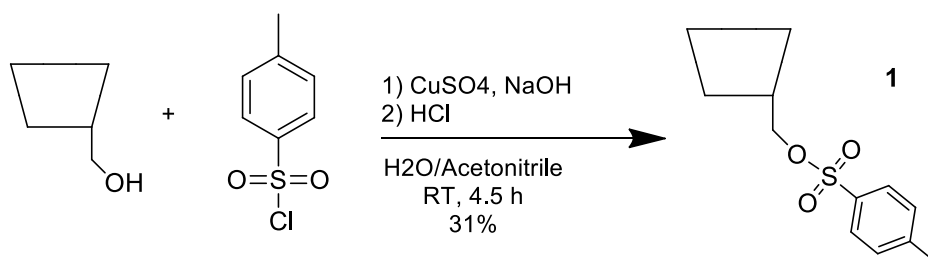
Figure 4.1. Synthesis of 6-O-Monotosyl-βCD.

4.2.1.2. 6-Monodeoxy-6-monoazido-βCD. This reaction was carried out according to literature [49]. TsOβCD (1.5 g, 1.16 mmol) and NaN$_3$ (378 mg, 5.82 mmol) were dissolved in DMF (9.3 mL). The mixture was stirred at 75°C for 24 hours. After, the mixture was precipitated in 200 mL acetone and filtered. Crude product was recrystallized in 11 mL water. This procedure was repeated until IR showed no peak from residual NaN$_3$ (2138 cm^{-1}). Pure product **2** was obtained as a white solid (1.202 g, 89%).
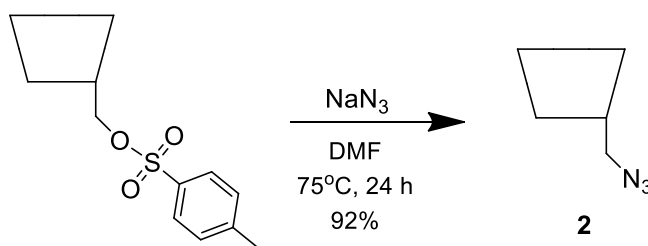
Figure 4.2. Synthesis of 6-Monodeoxy-6-monoazido-βCD.

4.2.1.3. DT40-Pent-4-ynoate (10%). This reaction was modified from literature [56]. DT40 (290 g, 1.62 mmol AHG) was weighed in a vial, sealed and purged with N$_2$ and dissolved in dry DMSO (1.6 mL). In a separate flask, 4-pentynoic acid (31.4 mg, 0.32 mmol), DPTS (14.4 mg, 0.049 mmol) and DCC (101 mg, 0.49 mmol) were purged with N$_2$ and dissolved in dry DMSO (1.6 mL). DT40 solution was added dropwise to 4-pentynoic acid solution. The mixture was stirred at RT for 24 hours. Formed N,N'-dicyclohexylurea salt was removed by filtration. Crude product was precipitated in cold IPA and removed by filtration. Presence of residual 4-pentynoic acid was monitored by TLC. Pure product **3** was obtained as a yellow solid (290 mg, 92%). ^{1}H-NMR (dDMSO, δ, ppm) 4.91 (bs, 1H, OH) 4.84 (m, 1H, CH anomeric proton) 4.68 (bs, 1H, OH), 4.47 (bs, 1H, OH) 3.74 (dd, 1H, -O-CH$_2$-) 3.64 (dt, 1H, O-CH-) 3.48 (overlap, 2H, -O-CH$_2$- (d) and –CH-OH (dd))

3.21 (overlap, 2H, -CH-OH (dd) and –CH-OR (dd)) 2.77 (s, 1H, ≡CH) 2.39 (t, 4H, O=C-CH₂-CH₂-)
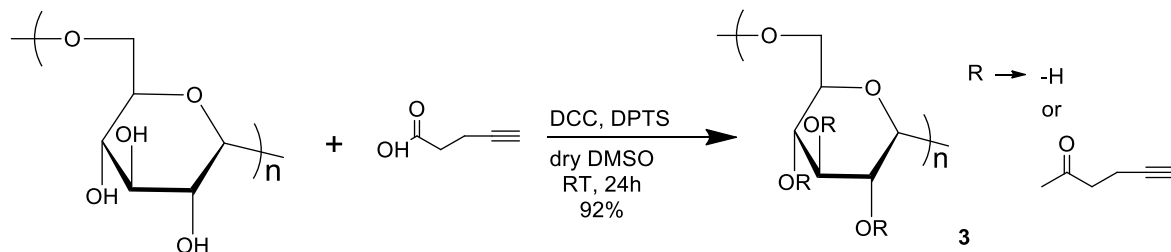
Figure 4.3. Synthesis of DT40-Pent-4-ynoate (10%).

4.2.1.4. DT40-βCD (10%). This reaction was modified from literature [53]. Cu(I)Br (9.9 g, 0.090 mmol) was weighed in the reaction flask and purged with N_2. DT40-Pent-4-noate **3** (100 g, 0.090 mmol alkyne) and $N_3βCD$ **2** (416 g, 0.360 mmol) were weighed in a vial and purged with N_2. PMDETA (18.8 μl, 0.090 mmol) was placed in a vial and purged with N_2. After 15 minutes, 10 mL dry DMF was divided between the three containers and purged for 10 minutes while mixing. PMDETA solution was added to Cu(I)Br solution and stirred for 5 minutes. Finally, DT40-Pent-4-noate and $N_3βCD$ solution was added to the reaction flask. The mixture was stirred at 50°C for 24h. Afterwards, DMF was evaporated on rotavap. Crude product was dissolved in minimum amount of water and dialyzed against water for 5 days (MWCO 10K) and lyophilized. Pure product was obtained as a white solid (127 mg, 69%). ^{1}H-NMR (dDMSO, δ, ppm) 7.81 (s , 1H, -N-CH=) 5.69 (bs, 14H, OH CD) 4.91 (bs, 1H, OH) 4.84 (m, 8H, CH anomeric proton dextran and CD) 4.68 (bs, 1H, OH), 4.48 (bs, 7H, OH dextran and CD) 3.74 (dd, 1H, -O-CH₂-) 3.64 (dt, 1H, O-CH-) 3.48 (overlap, 2H, -O-CH₂- (d) and –CH-OH (dd)) 3.21 (overlap, 2H, -CH-OH (dd) and –CH-OR (dd))
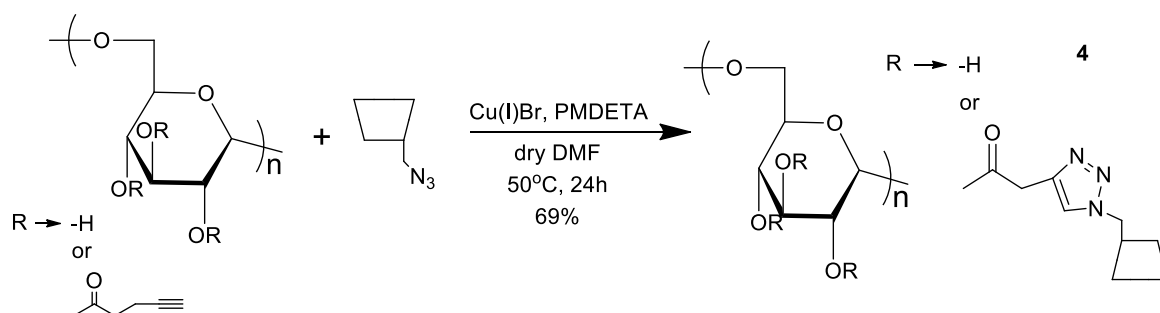
Figure 4.4. Synthesis of DT40-βCD.

4.2.2. Synthesis of Bis-AD Linkers

4.2.2.1. Disulfide containing bis-AD linker (first generation). 1-adamantane methanol **5** (250 mg, 1.5 mmol), 4,4-dithiodibutyric acid (1072 mg, 4.5 mmol), EDCI (633 mg, 3.3 mmol) and DMAP (36.6 mg, 0.3 mmol) were weighed in the reaction flask and purged with N_2 for 10 minutes. Dry DCM (14 mL) was added to the flask and the mixture was stirred for 20 hours at RT. After, reaction mixture was dissolved in 60 mL DCM and extraction was done with 60 mL saturated $NaHCO_3$ solution 3 times. Organic layer was dried over Na_2SO_4. Crude product was purified by column chromatography. Pure AD-SS-AD **5** was obtained as white solid (79 mg, 10%). ^{1}H-NMR (CDCl$_3$, δ, ppm) 3.68 (d, 4H, -CH$_2$-O-) 2.73 (t, 4H, J = 6.8 Hz, -CH$_2$-S-) 2.46 (t, 4H, J = 7.0 Hz, O=C-CH$_2$-) 2.02 (overlap, 4H, -CH$_2$- (tt, J = 17.5, 10.5 Hz), 6H, CH AD (m)) 1.69 (dd, 12H, J = 33.4, 11.8 Hz, -CH$_2$- AD) 1.52 (d, 12H, -CH$_2$- AD). ^{13}C-NMR (CDCl$_3$, δ, ppm) 173.2 (2C) 74.2 (2C) 39.4 (6C) 38.0 (2C) 37.1 (6C) 33.3 (2C) 32.8 (4C) 28.2 (6C) 24.4 (2C). FTIR 1727 cm^{-1} (C=O) 1203 (C-O-C)
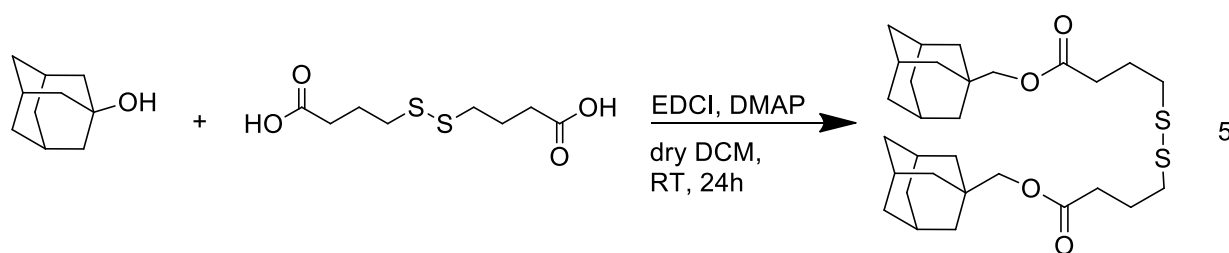
Figure 4.5. Synthesis of disulfide containing bis-AD linker.

4.2.2.2. AD-TEG. To 10 mL tetraethyleneglycol (TEG) (11.265 g, 58 mmol), 1-Bromoadamantane (500 mg, 2.32 mmol) and TEA (71 mg, 0.702 mmol) was added. The mixture was stirred at 120°C for 48 hours. Rection mixture was dissolved in 30 mL DCM and extraction was done with 1 M HCl (3 x 30 ml) and water (3 x 30 mL). Organic layer was dried over Na_2SO_4. Crude product was purified by column chromatography. Pure product **6** was obtained as a yellowish liquid (392 mg, 51%).
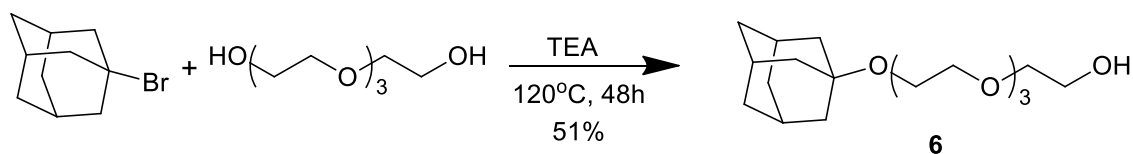
Figure 4.6. Synthesis of AD-TEG.

4.2.2.3. Disulfide containing bis-AD-TEG linker (second generation). AD-TEG **5** (400 mg, 1.22 mmol), 4,4-dithiodibutyric acid (194 mg, 0.81 mmol), EDCI (341 mg, 1.78 mmol) and DMAP (19.5 mg, 0.16 mmol) were weighed in the reaction flask and purged with N_2 for 10 minutes. Dry DCM (5.9 mL) was added to the flask and the mixture was stirred for 20 hours at RT. After, reaction mixture was dissolved in 60 mL DCM and extraction was done with 40 mL saturated $NaHCO_3$ solution 3 times. Organic layer was dried over Na_2SO_4. Crude product was purified by column chromatography. Pure AD-TEG-SS-TEG-AD **7** was obtained as a yellow liquid (254 mg, 24%). ^{1}H-NMR (CDCl$_3$, δ, ppm) 4.23 (t, 4H, J = 10.2 Hz, -CH$_2$-O-C=O) 3.69 (t, 4H, -CH$_2$-O-) 3.67-3.54 (m, -O-CH$_2$-CH$_2$-O- TEG) 2.71 (t, 4H, J = 7.1 Hz, -CH$_2$-S-) 2.47 (t, 4H, J = 7.3 Hz, -CH$_2$-C=O) 2.13 (m, 6H, CH AD) 2.02 (tt, 4H, J = 7.2 Hz, -CH$_2$-) 1.74 (d, 12H, J = 2.7 Hz, -CH$_2$- AD) 1.60 (dd, 12H, J = 12.3 Hz, -CH$_2$- AD). ^{13}C-NMR (CHCl$_3$, δ, ppm) 173.0 (2C) 72.4 (2C) 71.4 (2C) 70.7 (8C) 69.2 (2C) 63.8 (2C) 59.4 (2C) 41.6 (6C) 37.8 (2C) 36.6 (6C) 32.6 (2C) 30.6 (6C) 24.2 (2C). FTIR 1732 cm^{-1} (C=O) 1183 (C-O-C)

Figure 4.7. Synthesis of disulfide containing bis-AD-TEG linker.

4.3. General Method for Blank Nanogel Formation

Various concentrations of DT40-βCD polymers in MQ water were prepared and stirred overnight to equilibrate. Solutions were then filtered (pore size 220 nm) before use. Stock solutions of bis-AD linker and bis-AD-TEG linker in MeOH were prepared.

4.3.1. First Generation Nanogels with bis-AD linker

Volume of solution needed to achieve known equivalents of βCD to AD was calculated and added to the polymer solution. The solution was stirred, oncovered, overnight under the fume hood to allow MeOH to evaporate and for the NGs to equilibrate.
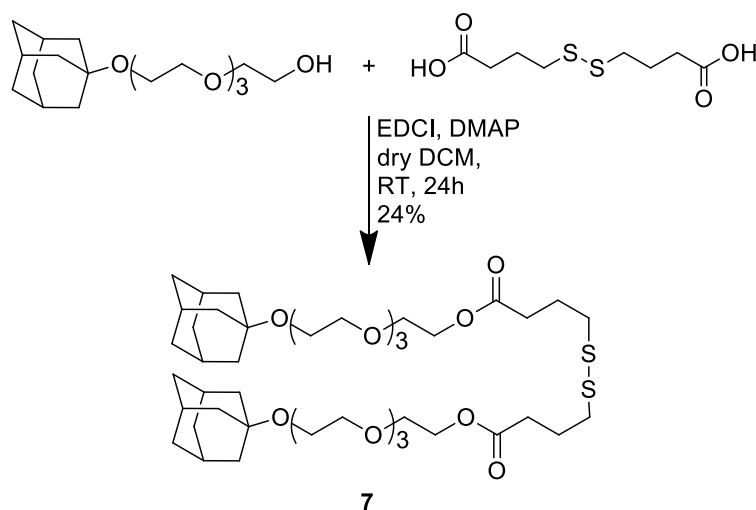
4.3.2. Second Generation Nanogels with bis-AD-TEG linker

Volume of solution needed to achieve known equivalents of βCD to AD was calculated, added to a vial and MeOH was evaporated under vacuum. The polymer solution was added the the same vial and stirred overnight for the NGs to equilibrate.

4.4. DOX Loaded Nanogel Formation

4.4.1. Mixing Method

1 mg/ml solution of DT40-βCD polymers in MQ water was prepared and stirred overnight to equilibrate. Solutions were then filtered (pore size 220 nm) before use. To this solution DOX.HCl was added and the mixture was sonicated for 2 hours. Volume of solution needed to achieve 1 equivalent of βCD to AD was calculated, added to a vial and MeOH was evaporated under vacuum. The polymer/DOX solution was added the the same vial and stirred overnight for the NGs to equilibrate.

4.4.2. Dialysis Method

5 mg of DT40-βCD, different equivalents of bis-AD-TEG linker, with different amounts of DOX.HCl with or without 20 equivalent TEA were dissolved in 1 mL DMSO and stirred overnight. Solution was added dropwise to varying amounts of MQ water and stirred for 30 minutes, then dialyzed against MQ water for 4.5 hours (MWCO 3500).

4.5.   Determination of Drug Loading and Loading Efficiency

Drug loading capacities (DL) and loading efficiencies (LE) of the NGs were determined using UV-Vis spectroscopy. To a 1 mL sample of NG solution in MQ water, 1 mL DMSO was added. The amount of drug present was determined by taking UV-Vis measurement at 485 nm and using a previously prepared calibration curve. DL and LE are defined below in Equations 4.1 and 4.2 respectively.

$$\text{DL} = \frac{\text{mg drug}}{\text{mg NG}} x 100 \tag{4.1}$$

$$\text{LE} = \frac{\text{mg drug}}{\text{mg feed}} x 100 \tag{4.2}$$

5. CONCLUSION

The aim of this study was the fabrication of biodegradable nangels that can be used as carriers for anti-cancer drugs using host-guest interactions between βCD and adamantane. The building blocks of the nanogel were βCD-grafted dextran and disulfide containing bis-adamantene linkers. Nanogels were formed simply by mixing the βCD functionalized dextran and bis-adamantane linkers together in water. βCD was attached to dextran by copper catalyzed azide alkyne cycloaddition ("click" reaction) due to its good yield and efficiency. The size and stability of the nanogels were found to be tunable by changing the polymer concentration and βCD to adamantane ratio. To observe the dissolution of the nanogels with reducing agent, DTT was added to nanogel solutions. For the first generation nanogels, no dissolution was observed. It was hypothesized that the steric hindrance and local hydrophobicity around the disulfide bond was preventing DTT from reaching it and a TEG spacer was added to the bis-adamantane linker. The second generation nanogels with bis-adamantane-TEG linker were responsive to addition of DTT and GSH and were chosen to continue on with drug loading studies.

Doxorubicin (DOX) was chosen as a model drug. DOX was loaded into the nanogels by simple mixing method and dialysis method. Mixing method did not produce stable nanogels within the acceptable size range (<200 nm). With the dialysis method, the size of the particles were tunable by changing the initial dilution and DOX loaded particles with acceptable size were obtained. Drug loading was 2.4 wt% and loading efficiency was 46%. An initial study of dissolution of DOX-loaded nanogels with DTT revealed that the NGs were responsive to high concentrations of DTT (100 mM) but not low (<10 mM). Further optimization studies will be carried out to fine tune the redox responsiveness to achieve dissembly at lower concentrations of thiol agents.
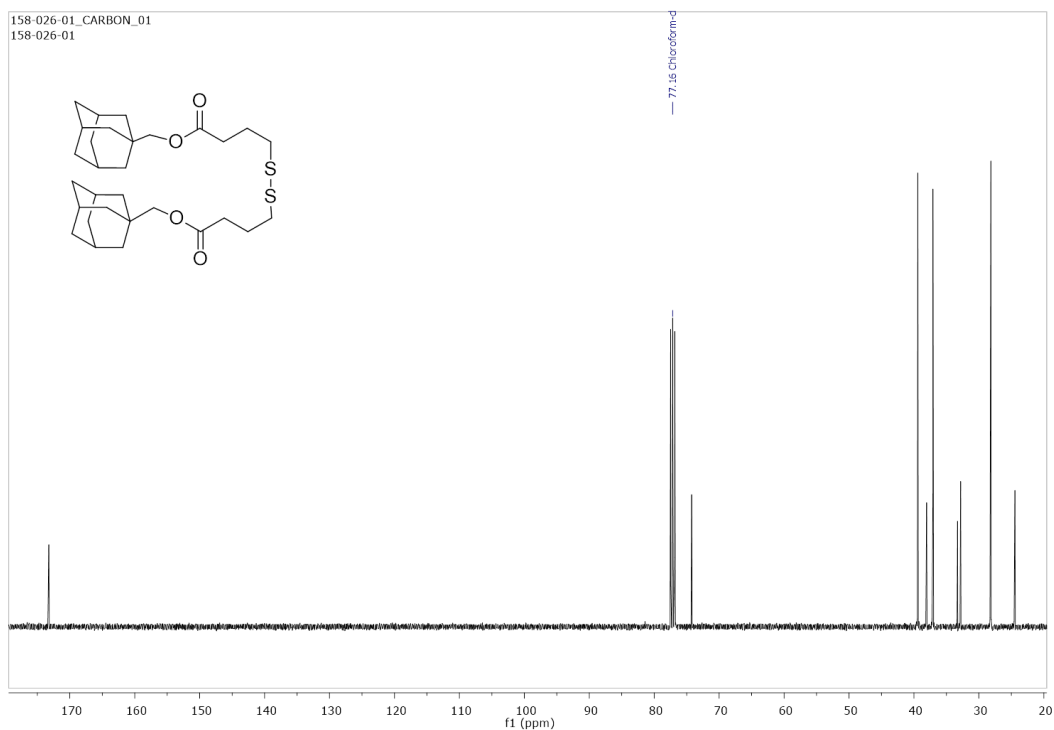
APPENDIX A: ^{13}C-NMR SPECTRA

Figure A.1. ^{13}C-NMR spectrum of bis-AD linker in CDCl$_3$.
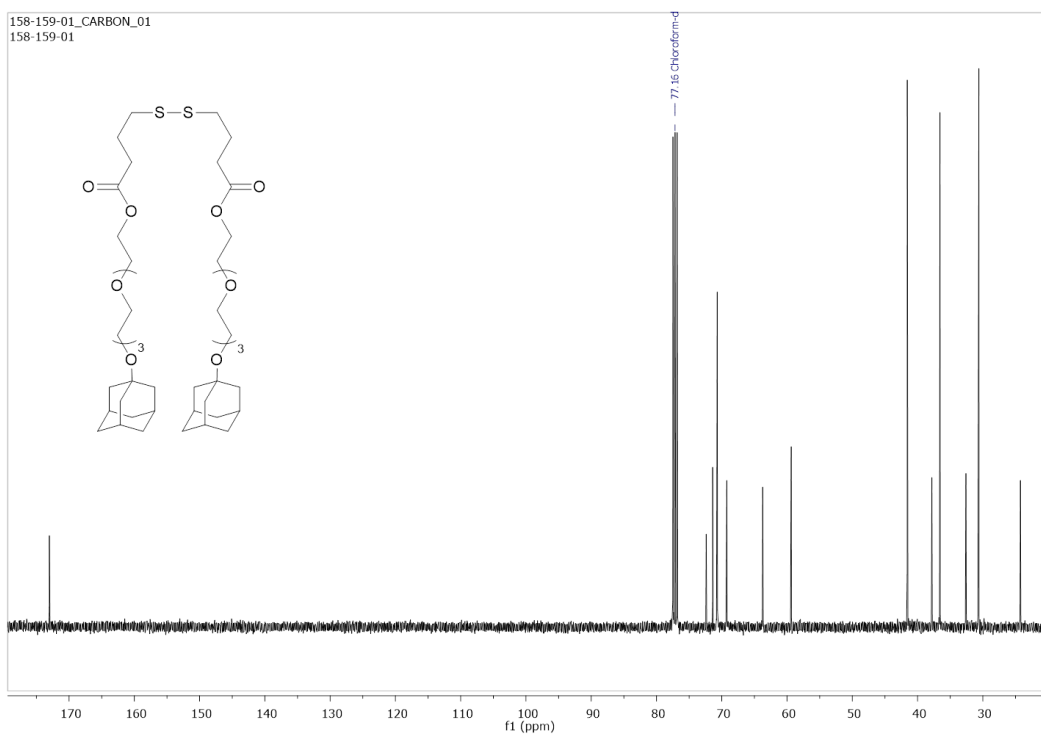

Figure A.2. ^{13}C-NMR spectrum of bis-AD-TEG linker in CDCl$_3$.

REFERENCES

1. Lehn, J.M., "Perspectives In Supramolecular Chemistry - From Molecular Recognition Towards Molecular Information Processing And Self-organization", *Angewandte Chemie - International Edition*, Vol. 29, pp. 1304–1319, 1990.

2. Steed, J.W., D.R. Turner, and K.J. Wallace, *Core Concepts in Supramolecular Chemistry and Nanochemistry*, John Wiley & Sons, Ltd., New York, 2007.

3. Whitesides, G.M. and B. Grzybowski, "Self-Assembly At All Scales", *Journal of the American Chemical Society*, Vol. 295, pp. 2418–2422, 2002.

4. Loftsson, T., and M.E. Brewster, "Pharmaceutical Applications Of Cyclodextrins: Basic Science And Product Development", *Journal of Pharmacy and Pharmacology*, Vol. 62, pp. 1607–1621, 2010.

5. Zhang, J., and P.X. Ma, "Cyclodextrin-based Supramolecular Systems For Drug Delivery: Recent Progress And Future Perspective", *Advanced Drug Delivery Reviews*, Vol. 65, pp. 1215–1233, 2013.

6. Szejtli, J., "Introduction And General Overview Of Cyclodextrin Chemistry", *Chemical Reviews*, Vol. 98, pp. 1743–1754, 1998.

7. Vyas, A., S. Saraf, and S. Saraf, "Cyclodextrin Based Novel Drug Delivery Systems", *Journal of Inclusion Phenomena and Macrocyclic Chemistry*, Vol. 62, pp. 23–42, 2008.

8. Irie, T., and K. Uekama, "Pharmaceutical Applications Of Cyclodextrins. III. Toxicological Issues And Safety Evaluation", *Journal of Pharmaceutical Sciences*, Vol. 86, pp. 147–162, 1997.

9. Loftsson, T., and D. Duchêne, "Cyclodextrins And Their Pharmaceutical Applications", *International Journal of Pharmaceutics*, Vol. 329, pp. 1–11, 2007.

10. Harada, A., Y. Takashima, and H. Yamaguchi, "Cyclodextrin-based Supramolecular Polymers", *Chemical Society Reviews*, Vol. 38, pp. 875–82, 2009.

11. Niu, Y., T. Huang, Z. Zhou, G. Xu, L. Zhang, and T. Wei, "Formation Of Cyclodextrin Monolayer Through A Host–guest Interaction With Tailor-made Phenyltriethoxysilane Self-assembled Monolayer", *Colloids and Surfaces A: Physicochemical and Engineering Aspects*, Vol. 470, pp. 224–229, 2015.

12. Collins, C.J., L.A. McCauliff, S.-H. Hyun, Z. Zhang, L.N. Paul, A. Kulkarni, K. Zick, M. Wirth, J. Storch, and D.H. Thompson, "Synthesis, Characterization, And Evaluation Of Pluronic-based B-cyclodextrin Polyrotaxanes For Mobilization Of Accumulated Cholesterol From Niemann-Pick Type C Fibroblasts", *Biochemistry*, Vol. 52, pp. 3242–53, 2013.

13. Daoud-Mahammed, S., P. Couvreur, and R. Gref, "Novel Self-assembling Nanogels: Stability And Lyophilisation Studies", *International Journal of Pharmaceutics*, Vol. 332, pp. 185–191, 2007.

14. Chen, M., S.R. Nielsen, T. Uyar, S. Zhang, A. Zafar, M. Dong, and F. Besenbacher, "Electrospun UV-responsive Supramolecular Nanofibers From A Cyclodextrin–azobenzene Inclusion Complex", *Journal of Materials Chemistry C*, Vol. 1, pp. 850–855, 2013.

15. He, Q., W. Wu, K. Xiu, Q. Zhang, F. Xu, and J. Li, "Controlled Drug Release System Based On Cyclodextrin-conjugated Poly(lactic Acid)-b-poly(ethylene Glycol) Micelles", *International Journal of pharmaceutics*, Vol. 443, pp. 110–9, 2013.

16. Voskuhl, J., U. Kauscher, M. Gruener, H. Frisch, B. Wibbeling, C.A. Strassert, and B.J. Ravoo, "A Soft Supramolecular Carrier With Enhanced Singlet Oxygen Photosensitizing Properties", *Soft Matter*, Vol. 9, pp. 2453, 2013.

17. Fülöp, Z., S.V. Kurkov, T.T. Nielsen, K.L. Larsen, and T. Loftsson, "Self-assembly Of Cyclodextrins: Formation Of Cyclodextrin Polymer Based Nanoparticles", *Journal of Drug Delivery Science and Technology*, Vol. 22, pp. 215–221, 2012.

18. Li, C., G.-F. Luo, H.-Y. Wang, J. Zhang, Y.-H. Gong, S.-X. Cheng, R.-X. Zhuo, and X.-Z. Zhang, "Host–Guest Assembly Of PH-Responsive Degradable Microcapsules With Controlled Drug Release Behavior", *The Journal of Physical Chemistry C*, Vol. 115, pp. 17651–17659, 2011.

19. Van de Manakker, F., T. Vermonden, N. El Morabit, C.F. van Nostrum, and W.E. Hennink, "Rheological Behavior Of Self-assembling PEG-beta-cyclodextrin/PEG-cholesterol Hydrogels", *Langmuir*, Vol. 24, pp. 12559–67, 2008.

20. Hu, Q. Da, G.P. Tang, and P.K. Chu, "Cyclodextrin-based Host-guest Supramolecular Nanoparticles For Delivery: From Design To Applications", *Accounts of Chemical Research*, Vol. 47, pp. 2017–2025, 2014.

21. Fujimoto, K., S. Yamada, and M. Inouye, "Synthesis Of Versatile Fluorescent Sensors Based On Click Chemistry: Detection Of Unsaturated Fatty Acids By Their Pyrene-emission Switching", *Chemical Communications*, pp. 7164–6, 2009.

22. Yan, Q., A. Feng, H. Zhang, Y. Yin, and J. Yuan, "Redox-switchable Supramolecular Polymers For Responsive Self-healing Nanofibers In Water", *Polymer Chemistry*, Vol. 4, pp. 1216–1220, 2013.

23. Chen, G., and M. Jiang, "Cyclodextrin-based Inclusion Complexation Bridging Supramolecular Chemistry And Macromolecular Self-assembly", *Chemical Society Reviews*, Vol. 40, pp. 2254–66, 2011.

24. Zhang, Z.-X., X. Liu, F.J. Xu, X.J. Loh, E.-T. Kang, K.-G. Neoh, and J. Li, "Pseudo-Block Copolymer Based On Star-Shaped Poly(N-isopropylacrylamide) With A B-Cyclodextrin Core And Guest-Bearing PEG: Controlling Thermoresponsivity Through Supramolecular Self-Assembly", *Macromolecules*, Vol. 41, pp. 5967–5970, 2008.

25. Kakuta, T., Y. Takashima, M. Nakahata, M. Otsubo, H. Yamaguchi, and A. Harada, "Preorganized Hydrogel: Self-healing Properties Of Supramolecular Hydrogels Formed By Polymerization Of Host-guest-monomers That Contain Cyclodextrins And Hydrophobic Guest Groups", *Advanced Materials*, Vol. 25, pp. 2849–2853, 2013.

26. Zhang, Z., J. Ding, X. Chen, C. Xiao, C. He, X. Zhuang, L. Chen, and X. Chen, "Intracellular PH-sensitive Supramolecular Amphiphiles Based On Host–guest Recognition Between Benzimidazole And B-cyclodextrin As Potential Drug Delivery Vehicles", *Polymer Chemistry*, Vol. 4, pp. 3265, 2013.

27. Zha, L., B. Banik, and F. Alexis, "Stimulus Responsive Nanogels For Drug Delivery", *Soft Matter*, Vol. 7, pp. 5908, 2011.

28. Kabanov, A. V., and S. V. Vinogradov, "Nanogels As Pharmaceutical Carriers: Finite Networks Of Infinite Capabilities", *Angewandte Chemie - International Edition*, Vol. 48, pp. 5418–5429, 2009.

29. Anil Kumar, S., and M.I. Khan, "Heterofunctional Nanomaterials: Fabrication, Properties And Applications In Nanobiotechnology", *Journal of Nanoscience and Nanotechnology*, Vol. 10, pp. 4124–4134, 2010.

30. Moya-Ortega, M.D., C. Alvarez-Lorenzo, A. Concheiro, and T. Loftsson, "Cyclodextrin-based Nanogels For Pharmaceutical And Biomedical Applications", *International Journal of Pharmaceutics*, Vol. 428, pp. 152–163, 2012.

31. Wintgens, V., S. Daoud-Mahammed, R. Gref, L. Bouteiller, and C. Amiel, "Aqueous Polysaccharide Associations Mediated By B-cyclodextrin Polymers", *Biomacromolecules*, Vol. 9, pp. 1434–1442, 2008.

32. Moya-Ortega, M.D., C. Alvarez-Lorenzo, H.H. Sigurdsson, A. Concheiro, and T. Loftsson, "Cross-linked Hydroxypropyl-β-cyclodextrin And Γ-cyclodextrin Nanogels For Drug Delivery: Physicochemical And Loading/release Properties", *Carbohydrate Polymers*, Vol. 87, pp. 2344–2351, 2012.

33. Kettel, M.J., F. Dierkes, K. Schaefer, M. Moeller, and A. Pich, "Aqueous Nanogels Modified With Cyclodextrin", *Polymer*, Vol. 52, pp. 1917–1924, 2011.

34. Wintgens, V., T.T. Nielsen, K.L. Larsen, and C. Amiel, "Size-Controlled Nanoassemblies Based On Cyclodextrin-Modified Dextrans", *Macromolecular Bioscience*, Vol. 11, pp. 1254–1263, 2011.

35. Wintgens, V., A.M. Layre, D. Hourdet, and C. Amiel, "Cyclodextrin Polymer Nanoassemblies: Strategies For Stability Improvement", *Biomacromolecules*, Vol. 13, pp. 528–534, 2012.

36. Daoud-Mahammed, S., C. Ringard-Lefebvre, N. Razzouq, V. Rosilio, B. Gillet, P. Couvreur, C. Amiel, and R. Gref, "Spontaneous Association Of Hydrophobized Dextran And Poly-B-cyclodextrin Into Nanoassemblies: Formation And Interaction With A Hydrophobic Drug", *Journal of Colloid and Interface Science*, Vol. 307, pp. 83–93, 2007.

37. Amiel, C., V. Wintgens, T.T. Nielsen, and K.L. Larsen, "Tailorable Polymeric Assemblies Based On Host/Guest Interactions Between Modified Dextrans", *Macromolecular Symposia*, Vol. 317-318, pp. 75–81, 2012.

38. Layre, A.M., G. Volet, V. Wintgens, and C. Amiel, "Associative Network Based On Cyclodextrin Polymer: A Model System For Drug Delivery", *Biomacromolecules*, Vol. 10, pp. 3283–3289, 2009.

39. Daoud-Mahammed, S., P. Couvreur, K. Bouchemal, M. Chéron, G. Lebas, C. Amiel, and R. Gref, "Cyclodextrin And Polysaccharide-based Nanogels: Entrapment Of Two Hydrophobic Molecules, Benzophenone And Tamoxifen", *Biomacromolecules*, Vol. 10, pp. 547–554, 2009.

40. Gref, R., C. Amiel, K. Molinard, S. Daoud-Mahammed, B. Sébille, B. Gillet, J.C. Beloeil, C. Ringard, V. Rosilio, J. Poupaert, and P. Couvreur, "New Self-assembled Nanogels Based On Host-guest Interactions: Characterization And Drug Loading", *Journal of Controlled Release*, Vol. 111, pp. 316–324, 2006.

41. Ang, C.Y., S.Y. Tan, X. Wang, Q. Zhang, M. Khan, L. Bai, S. Tamil Selvan, X. Ma, L. Zhu, K.T. Nguyen, N.S. Tan, and Y. Zhao, "Supramolecular Nanoparticle Carriers

Self-assembled From Cyclodextrin- And Adamantane-functionalized Polyacrylates For Tumor-targeted Drug Delivery", *Journal of Materials Chemistry B*, Vol. 2, pp. 1879, 2014.

42. Zan, M., J. Li, S. Luo, and Z. Ge, "Dual PH-triggered Multistage Drug Delivery Systems Based On Host-guest Interaction-associated Polymeric Nanogels.", *Chemical Communications*, Vol. 50, pp. 7824–7, 2014.

43. Chen, X., L. Chen, X. Yao, Z. Zhang, C. He, J. Zhang, and X. Chen, "Dual Responsive Supramolecular Nanogels For Intracellular Drug Delivery", *Chemical Communications*, Vol. 50, pp. 3789–91, 2014.

44. Kolb, H.C., M.G. Finn, and K.B. Sharpless, "Click Chemistry: Diverse Chemical Function From A Few Good Reactions", *Angewandte Chemie - International Edition,* Vol 40, pp. 2004-2021, 2001.

45. Rostovtsev, V. V, L.G. Green, V. V Fokin, and K.B. Sharpless, "A Stepwise Huisgen Cycloaddition Process: Copper(I)-catalyzed Regioselective 'Ligation' Of Azides And Terminal Alkynes", *Angewandte Chemie - International Edition*, Vol. 41, pp. 2596–2599, 2002.

46. Tornøe, C.W., C. Christensen, and M. Meldal, "Peptidotriazoles On Solid Phase: [1,2,3]-Triazoles By Regiospecific Copper(I)-Catalyzed 1,3-Dipolar Cycloadditions Of Terminal Alkynes To Azides", *The Journal of Organic Chemistry*, Vol. 67, pp. 3057–3064, 2002.

47. Hein, J.E., and V. V Fokin, "Copper-catalyzed Azide-alkyne Cycloaddition (CuAAC) And Beyond: New Reactivity Of Copper(I) Acetylides", *Chemical Society Reviews*, Vol. 39, pp. 1302–1315, 2010.

48. Traverso, N., R. Ricciarelli, M. Nitti, B. Marengo, A.L. Furfaro, M.A. Pronzato, U.M. Marinari, and C. Domenicotti, "Role Of Glutathione In Cancer Progression And Chemoresistance", *Oxidative Medicine and Cellular Longevity*, Vol. 2013 2013.

49. Nielsen, T.T., V. Wintgens, C. Amiel, R. Wimmer, and K.L. Larsen, "Facile Synthesis Of Beta-cyclodextrin-dextran Polymers By 'Click' Chemistry", *Biomacromolecules*, Vol. 11, pp. 1710–1715, 2010.

50. Baussanne, I., H. Law, J. Defaye, J.M. Benito, C.O. Mellet, and J.M. García Fernández, "Synthesis And Comparative Lectin-binding Affinity Of Mannosyl-coated B-cyclodextrin-dendrimer Constructs", *Chemical Communications*, Vol. 8, pp. 1489–1490, 2000.

51. Tripodo, G., C. Wischke, A.T. Neffe, and A. Lendlein, "Efficient Synthesis Of Pure Monotosylated Beta-cyclodextrin And Its Dimers", *Carbohydrate Research*, Vol. 381, pp. 59–63, 2013.

52. Peng, K., I. Tomatsu, A. V. Korobko, and A. Kros, "Cyclodextrin–dextran Based In Situ Hydrogel Formation: A Carrier For Hydrophobic Drugs", *Soft Matter*, Vol. 6, pp. 85–87, 2010.

53. Schmidt, B.V.K.J., M. Hetzer, H. Ritter, and C. Barner-Kowollik, "Miktoarm Star Polymers Via Cyclodextrin-driven Supramolecular Self-assembly", *Polymer Chemistry*, Vol. 3, pp. 3064, 2012.

54. Saenger, W., "Crystal Packing Patterns Of Cyclodextrin Inclusion Complexes", *Journal of Inclusion Phenomena*, Vol. 2, pp. 445–454, 1984.

55. Swiech, O., a Mieczkowska, K. Chmurski, and R. Bilewicz, "Intermolecular Interactions Between Doxorubicin And Beta-cyclodextrin 4-methoxyphenol Conjugates", *Journal of Physical Chemistry B*, Vol. 116, pp. 1765–1771, 2012.

56. Peng, K., I. Tomatsu, A. V. Korobko, and A. Kros, "Cyclodextrin–dextran Based In Situ Hydrogel Formation: A Carrier For Hydrophobic Drugs", *Soft Matter*, Vol. 6, pp. 85, 2010.